

 Open access • Posted Content • DOI:10.1101/2020.09.15.20188896

Pre-existing T cell memory as a risk factor for severe 1 COVID-19 in the elderly

— [Source link](#) 

Petra Bacher, Elisa Rosati, Daniela Esser, Gabriela Rios Martini ...+22 more authors

Institutions: University of Kiel, Goethe University Frankfurt, University of Cologne

Published on: 18 Sep 2020 - medRxiv (Cold Spring Harbor Laboratory Press)

Topics: T cell, Avidity and T-cell receptor

Related papers:

- [SARS-CoV-2-specific T cell immunity in cases of COVID-19 and SARS, and uninfected controls.](#)
- [Targets of T Cell Responses to SARS-CoV-2 Coronavirus in Humans with COVID-19 Disease and Unexposed Individuals.](#)
- [Selective and cross-reactive SARS-CoV-2 T cell epitopes in unexposed humans.](#)
- [Robust T Cell Immunity in Convalescent Individuals with Asymptomatic or Mild COVID-19.](#)
- [Pre-existing immunity to SARS-CoV-2: the knowns and unknowns.](#)

Share this paper:    

View more about this paper here: <https://typeset.io/papers/pre-existing-t-cell-memory-as-a-risk-factor-for-severe-1-196be0ylnh>

1 **Pre-existing T cell memory as a risk factor for severe COVID-19 in the elderly**

2
3 Petra Bacher,^{1,2,14} Elisa Rosati², Daniela Esser³, Gabriela Rios Martini,^{1,2} Carina Saggau¹,
4 Esther Schiminsky¹, Justina Dargvainiene³, Ina Schöder³, Imke Wieters⁴, Yascha
5 Khodamoradi⁴ Fabian Eberhardt⁴, Holger Neb⁵, Michael Sonntagbauer⁵, Maria J.G.T.
6 Vehreschild⁴, Claudio Conrad⁶, Florian Tran^{2,7}, Philip Rosenstiel², Robert Markewitz⁸, Klaus-
7 Peter Wandinger⁸, Jan Rybniker^{9,10,11}, Matthias Kochanek⁹, Frank Leypoldt³, Oliver A.
8 Cornely^{9,10,11,12,13}, Philipp Koehler^{9,10,13}, Andre Franke² and Alexander Scheffold¹

9
10 ¹Institute of Immunology, Christian-Albrechts-University of Kiel & UKSH Schleswig-Holstein,
11 Kiel, Germany

12 ²Institute of Clinical Molecular Biology, Christian-Albrechts-University of Kiel, Kiel, Germany.

13 ³Neuroimmunology, Institute of Clinical Chemistry, University Hospital Schleswig-Holstein,
14 Kiel, Germany

15 ⁴Department of Internal Medicine, Infectious Diseases, University Hospital Frankfurt & Goethe
16 University Frankfurt, Frankfurt am Main, Germany.

17 ⁵Department of Anesthesiology, Intensive Care Medicine and Pain Therapy, University
18 Hospital Frankfurt, Frankfurt am Main, Germany.

19 ⁶Department of Internal Medicine, Hospital of Preetz, Preetz, Germany

20 ⁷ Department of Internal Medicine I, UKSH Kiel, Germany

21 ⁸Institute of Clinical Chemistry, University Hospital Schleswig-Holstein, Lübeck, Germany

22 ⁹University of Cologne, Medical Faculty and University Hospital Cologne, Department I of
23 Internal Medicine, 50937 Cologne, Germany

24 ¹⁰Center for Molecular Medicine Cologne (CMMC), University of Cologne, 50931, Cologne,
25 Germany

26 ¹¹University of Cologne, Medical Faculty and University Hospital Cologne, German Center for
27 Infection Research (DZIF), Partner Site Bonn-Cologne, 50937 Cologne, Germany.

28 ¹²Clinical Trials Centre Cologne, ZKS Köln, 50935 Cologne, Germany.

29 ¹³University of Cologne, Cologne Excellence Cluster on Cellular Stress Responses in Aging-
30 Associated Diseases (CECAD), 50937 Cologne, Germany

31 ¹⁴Lead contact

32 **Corresponding Author**

33 Petra Bacher

34 Christian-Albrechts Universität zu Kiel & Universitätsklinik Schleswig-Holstein

35 Institute of Immunology & Insitute of Clinical Molecular Biology

36 Arnold-Heller-Str. 3, 24105 Kiel, Germany

37 Phone: +49 (0) 431 500-31005

38 Fax: +49 (0) 431 500-31004

39 Email: p.bacher@ikmb.uni-kiel.de

NOTE: This preprint reports new research that has not been certified by peer review and should not be used to guide clinical practice.

39 **Summary**

40
41 Coronavirus disease 2019 (COVID-19) displays high clinical variability but the parameters that
42 determine disease severity are still unclear. Pre-existing T cell memory has been hypothesized
43 as a protective mechanism but conclusive evidence is lacking. Here we demonstrate that all
44 unexposed individuals harbor SARS-CoV-2-specific memory T cells with marginal cross-
45 reactivity to common cold corona and other unrelated viruses. They display low functional
46 avidity and broad protein target specificities and their frequencies correlate with the overall
47 size of the CD4+ memory compartment reflecting the “immunological age” of an individual.
48 COVID-19 patients have strongly increased SARS-CoV-2-specific inflammatory T cell
49 responses that are correlated with severity. Strikingly however, patients with severe COVID-
50 19 displayed lower TCR functional avidity and less clonal expansion. Our data suggest that a
51 low avidity pre-existing T cell memory negatively impacts on the T cell response quality against
52 neoantigens such as SARS-CoV-2, which may predispose to develop inappropriate immune
53 reactions especially in the elderly. We propose the immunological age as an independent risk
54 factor to develop severe COVID-19.

55

56

57 **Key points**

58 - Pre-existing SARS-CoV-2-reactive memory T cells are present in all humans, but have low
59 functional avidity and broad target specificities

60

61 - Pre-existing memory T cells show only marginal cross-reactivity to common cold corona
62 viruses

63

64 - Frequencies of pre-existing memory T cells increase with the size of the CD4+ memory
65 compartment reflecting the “immunological age” of the individual

66

67 - Low-avidity and polyclonal, but strongly enhanced SARS-CoV-2 specific T cell responses
68 develop in severe COVID-19, suggesting their origin from pre-existing memory

69

70 - The immunological age may represent a risk factor to develop severe COVID-19

71 **Introduction**

72 COVID-19 displays remarkable disparity of clinical symptoms, ranging from asymptomatic or
73 mild disease frequently observed in children and younger adults to severe clinical symptoms
74 associated with high mortality mainly in elderly and high-risk patients. Differences in the
75 immune response may contribute to this diverse pathology. Severe disease is characterized
76 by hyperinflammation, suggesting that exaggerated immune reactions are part of COVID-19
77 pathogenesis. However, it is currently not clear which type of adaptive immunity to SARS-CoV-
78 2 is protective or detrimental. Thus, there is an enormous interest to decipher the anti-SARS-
79 CoV-2 response, both to define parameters of immune protection *versus* pathology, as well as
80 for the design of effective vaccination strategies.

81 SARS-CoV-2-specific CD4⁺ T cells are prime candidates to be involved in this process. They
82 are central organizers of anti-viral immune responses while uncontrolled T cell responses may
83 cause pathology. Severe lymphopenia accompanies severe disease and T cell reappearance
84 correlates with patient recovery (Huang et al., 2020; Tan et al., 2020; Wang et al., 2020; Yang
85 et al., 2020). Markers of T cell activation were found to be increased on total (Diao et al., 2020;
86 Sekine et al., 2020; Wilk et al., 2020; Zheng et al., 2020), as well as on SARS-CoV-2-specific
87 T cells (Braun et al., 2020; Sekine et al., 2020). Overall COVID-19 patients seem to develop
88 robust Th1-like SARS-CoV-2-specific CD4⁺ T cell responses focused on spike, membrane
89 and nucleocapsid (Ncap) proteins (Grifoni et al., 2020). Increased frequencies of SARS-CoV-
90 2-specific T cells have been correlated with more severe disease (Anft et al., 2020; Peng et
91 al., 2020) supporting the idea that exaggerated CD4⁺ T cell responses may contribute to the
92 hyperinflammation. However, the factors which determine the magnitude as well as the quality
93 of the CD4⁺ T cell response and how this relates to predisposition and/ or manifestation of
94 severe disease remains unknown. In particular, the effect of aging is discussed, since the risk
95 to develop severe COVID-19 dramatically increases in the elderly.

96 Several studies have observed that a certain fraction of un-exposed donors have pre-existing
97 SARS-CoV-2-reactive T cells (Braun et al., 2020; Grifoni et al., 2020; Le Bert et al., 2020;
98 Mateus et al., 2020; Meckiff et al., 2020; Sekine et al., 2020; Weiskopf et al., 2020) which
99 contained at least some T cells cross-reactive against selected peptides with homology to
100 related common cold corona virus strains (CCCoV) (Braun et al., 2020; Mateus et al., 2020).
101 From this it was hypothesized that encounter with CCCoV may provide protective cross-
102 reactive memory especially in younger patients, where infections with CCCoV are especially
103 prevalent.

104 However, data on the prevalence of CD4⁺ T cell responses against CCCoV in humans are
105 lacking. Furthermore, pre-existing immunity has also been described for several other
106 pathogens and neoantigens (Bacher et al., 2013; Campion et al., 2014; Kwok et al., 2012; Su
107 et al., 2013) with variable consequences, from protective to harmful (Bacher et al., 2019;

108 Greiling et al., 2018; Koutsakos et al., 2019; Sridhar et al., 2013; Welsh et al., 2010; Woodland
109 and Blackman, 2006). Thus its impact may depend on the T cells functional characteristics,
110 the specific antigen- or pathogen-context (Sette and Crotty, 2020), and age (Woodland and
111 Blackman, 2006). Such functional characteristics of SARS-CoV-2-specific T cells in severe
112 *versus* mild COVID-19 and unexposed individuals are still poorly described. Specifically, the
113 prevalence of the putative cross-reactive T cells within unexposed donors and COVID-19
114 patients and in different age groups, their phenotypic and functional characteristics, as well as
115 the inducing antigen(s) are unknown.

116 Here we show that pre-existing memory T cells are present in all unexposed donors and
117 increased in the elderly, but not primarily driven by CCCoVs. Pre-existing SARS-CoV-2-
118 specific memory T cells possess only low TCR avidity, suggesting impaired functionality. This
119 functional impairment is closely mirrored in T cells from severe COVID-19 patients in contrast
120 to mild disease, suggesting that they may originate from pre-existing memory T cells. Thus we
121 suggest the immunological age as a potential risk factor for severe COVID-19.

122

123 **Results**

124

125 **Strongly increased frequencies of human SARS-CoV-2-reactive CD4+ T cells against** 126 **the spike, membrane and Ncap proteins in COVID-19 patients**

127

128 To characterize the human T cell response against SARS-CoV-2, we analyzed T cells reactive
129 against a panel of 12 different SARS-CoV-2 proteins. SARS-CoV-2-reactive CD4+ T cells were
130 detected based on the up-regulation of CD154+ (CD40L) following 7h ex vivo stimulation of
131 PBMCs with overlapping peptide pools of the different proteins and subsequent magnetic
132 enrichment (Antigen-reactive T cell enrichment, ARTE) (Bacher et al., 2016; Bacher et al.,
133 2019) (Figure S1A). SARS-CoV-2 exposure *versus* non-exposure of blood donors was verified
134 by SARS-CoV-2 PCR and/ or serology testing (Table S1).

135 The response of COVID-19 patients was mainly directed against three proteins, spike,
136 membrane and nucleocapsid (Ncap), as previously suggested (Grifoni et al., 2020), as well as
137 to lower extent and with more variability between donors against AP3a, ORF9b, NS6, NS7a
138 and NS8 (Figure 1A, B). We observed no differences in the reactivity against the N-terminal or
139 C-terminal part of the spike protein in COVID-19 patients. The frequencies of reactive cells
140 against single or pooled spike, membrane and Ncap, were strongly increased in patients
141 *versus* unexposed individuals (Figure 1C), whereas no differences were detected against a
142 pool of Influenza A H1N1 proteins (containing HA, MP1, MP2, NP and NA), as a control
143 antigen. In contrast to previous reports suggesting pre-existing memory only in a subset of
144 unexposed individuals, the sensitive detection by ARTE identified SARS-CoV-2 reactive T cells
145 in all unexposed donors albeit at low and variable frequencies ranging from 1 in 10^{-5} - 10^{-3}
146 (Figure 1A-C). However, while typically >80-90% of SARS-CoV-2 reactive T cells in COVID-
147 19 patients were directed against spike, membrane and Ncap, the response in unexposed
148 donors was much more variable and directed against multiple proteins (Figure 1D) (Grifoni et
149 al., 2020; Le Bert et al., 2020). The specificity of the SARS-CoV-2-reactive cells in unexposed
150 as well as exposed donors was confirmed by high reactivity of sorted and expanded CD154+
151 T cells towards SARS-CoV-2, but not control antigens (Figure S1B, C).

152

153

154

155 **SARS-CoV-2 reactive T cells of COVID-19 patients show an activated Th1/Tfh-like** 156 **signature**

157

158 SARS-CoV-2 reactive cells from COVID-19 patients *versus* unexposed individuals displayed
159 increased expression of the acute and chronic activation markers Ki-67 and CD38 (Figure 2A),
160 as reported by others (Braun et al., 2020; Sekine et al., 2020). The expression of both markers
161 declined with time after infection, but not the frequencies of reactive T cells (Figure 2B, C). We
162 also detected slightly increased relative and strongly increased absolute production of
163 inflammatory cytokines in COVID-19 patients, such as IL-2, IFN- γ and IL-21 compared to

164 unexposed donors, as well as a slightly higher production of IL-10 (Figure 2D, E). While
165 inflammatory cytokines increased with time after infection, IL-10 was mainly produced during
166 active disease (Figure S2A), suggesting a counter-regulatory mechanism during acute
167 infection. In addition, SARS-CoV-2 reactive T cells expressed stably high levels of PD-1
168 (CD279) (Figure 2D, E and S2A). Compared to other anti-viral responses, production of TNF-
169 α , IFN- γ and IL10 was rather reduced in convalescent COVID-19 patients, while IL-21 and PD-
170 1 were highly increased (Figure 2F, Figure S2B). We observed no differences in the cytokine
171 response or phenotype between the individual SARS-CoV-2 proteins (Figure 2F, Figure S2B).
172

173 **Single-cell RNA sequencing identifies similar T cell clusters in COVID-19 and** 174 **unexposed donors** 175 176

177 To obtain a deeper insight into the cellular composition of SARS-CoV-2-specific T cells and
178 their molecular patterns we next performed single-cell RNA sequencing of *ex vivo* FACS-
179 purified SARS-CoV-2 reactive memory T cells. After quality filtering (see Methods) we
180 analyzed in total 104,417 single cells from 6 unexposed and 14 COVID-19 patients.

181 UMAP cluster analysis revealed five clusters with a distinct transcriptional profile (Figure 3A).
182 These were assigned as T follicular-helper-like (Tfh-like, key marker genes *IL21*, *POU2AF1*),
183 transitional memory (*CD28*, *IL7R*), central memory (*CCR7*, *SELL*), cytotoxic (*IFNG*, *CSF2*,
184 *PRF1*, *GNLY*), type-I interferon response (*MX1*, *OAS1*) and cycling T cells (*MKI67*, *CDK1*)
185 (Figure 3B). Similar clusters have recently been described in anti-viral T cells (Meckiff et al.,
186 2020). However, especially Tfh-like, transitional and central memory T cells were related and
187 important genes like *IFNG*, *CSF2*, *IL21*, *IL2* and *PDCD1* were expressed by many cells in all
188 clusters although at different level (Figures 3B, Figure S3A). In addition, we observed three
189 robust clusters, cytotoxic /Th1, type-I interferon, and cycling, which are indicative of cellular
190 activation and an anti-viral type-I interferon response. These results confirm our cytometric
191 analysis pointing to a highly activated Th1 and Tfh-like phenotype of SARS-CoV-2 specific T
192 cells in COVID-19. However, similar clusters were also identified in SARS-CoV-2 reactive
193 memory T cells from unexposed individuals and we were not able to clearly separate
194 unexposed donors from COVID-19 patients or between patients with different disease severity
195 only based on qualitative differences of the reactive T cells (Figure 3C, Figure S3B). There was
196 a tendency that clusters indicative of acute activation, such as cycling and type-I interferon
197 were relatively enriched in COVID-19 and Tfh cells were more abundant in mild COVID19
198 (Figure 3C).

199 Taken together, the cytometric and single cell sequencing data confirm that COVID-19 patients
200 generate a strong pro-inflammatory Th1/cytotoxic-like and Tfh-like response against SARS-
201 CoV-2 spike, membrane, and Ncap proteins. Interestingly though, the differences between the

202 patients groups and healthy controls were mainly quantitative, rather than qualitative. This
203 suggests that these cell types are not unique to COVID-19 but may represent a common
204 cellular phenotype of anti-viral T cells, which are already present in pre-existing SARS-CoV-2-
205 reactive memory T cells from healthy unexposed donors.

206
207

208 **Low avidity SARS-CoV-2-reactive memory T cells increase with age in unexposed** 209 **donors**

210 Recent studies have demonstrated pre-existing T cell immunity against SARS-CoV-2
211 presumably against common cold viruses in 20-50% of unexposed donors (Braun et al., 2020;
212 Grifoni et al., 2020; Le Bert et al., 2020; Mateus et al., 2020; Meckiff et al., 2020; Sekine et al.,
213 2020; Weiskopf et al., 2020). However, the antigen specificity as well as the clinical relevance
214 of this cross-reactivity remains unknown (Sette and Crotty, 2020) although some cross-
215 reactivity against homologous CCCoV epitopes has been found (Braun et al., 2020; Mateus et
216 al., 2020). As shown in Figure 1, by sensitive enrichment of reactive T cells we detected low
217 frequencies of cross-reactive T cells against different SARS-CoV-2 proteins in 100% of
218 unexposed donors. To further characterize these pre-existing SARS-CoV-2-reactive T cells,
219 we determined the proportion of memory *versus* naïve cells. Remarkably, a substantial fraction
220 of SARS-CoV-2-reactive cells from unexposed donors but not COVID-19 patients displayed a
221 naïve phenotype, as evidenced by high expression of CD45RA and CCR7 and lack of effector
222 cytokine expression (Figure 4A, B; Figure 2F). The proportion of memory cells was highly
223 variable between different donors (range 25-95%) (Figure 4B). It has further been speculated
224 that this pre-existing immunity may improve protection especially in young patients and
225 children due to frequent infections with common cold corona viruses (Braun et al., 2020).
226 However, we detected no correlation of pre-existing T cell frequency with donor age (Figure
227 4C). Rather and in sharp contrast to the “pre-immune” hypothesis, the frequency (Figure 4D)
228 and the proportion (Figure 4E) of SARS-CoV-2 cross-reactive memory cells of unexposed
229 individuals positively correlated with the proportion of memory cells within the total CD4+
230 population that is associated to the immunological age. A similar pattern was observed for
231 CMV-reactive T cells from CMV sero-negative *versus* sero-positive donors (Figure 4E), as well
232 as T cells reactive against the neoantigen keyhole limpet hemocyanin (KLH) (Figure S4).
233 These data argue against induction of the pre-existing SARS-CoV-2 memory cells by a specific
234 cross-reactive antigen, but rather for arbitrary stochastic selection from a large memory
235 repertoire in adult humans. In support of this, SARS-CoV-2-reactive memory T cells expanded
236 from unexposed individuals displayed a 1-2 log lower functional avidity compared to COVID-
237 19 patients, which was in the same range as CMV-reactive T cells (Figure 4F, G). Taken
238 together, pre-existing SARS-CoV-2 cross-reactive memory T cells in unexposed donors are

239 common in humans and increase with the immunological age but do not display features of a
240 protective cross-reactive T cell population.

241

242 **Robust memory T cell response to common cold corona viruses (CCCoVs)**

243 Our data do not exclude the possibility that in some donors protective pre-existing immunity
244 may exist, for example due to infections with related common cold corona viruses (CCCoVs).
245 Since data on the prevalence of CCCoV-specific T cell memory are lacking, we next analysed
246 the response against spike proteins from the CCCoV strains 229E, OC43, HKU1 and NL63.
247 Strikingly, robust memory T cell responses were readily detected in all donors with frequencies
248 ranging between 1 in 10^3 - 10^4 (Figure 5A, B), which is in a similar range like against Influenza
249 A (Figure 1C), but up to 10-fold higher than SARS-CoV-2 spike-reactive T cells (Figure 5B).
250 CCCoV responses displayed a memory phenotype (Figure 5C, D), independent of
251 immunological age (Figure S5A), and high functional avidity (Figure 5E) in accordance with an
252 *in vivo* induction upon viral infection. Of note, expanded CCCoV-specific T cells from healthy
253 donors showed only marginal cross-reactivity against SARS-CoV-2 spike protein and *vice*
254 *versa* (Figure 5F, G). Furthermore, while the frequencies of reactive memory T cells between
255 the different CCCoVs showed strong linear correlation as an indicator of cross-recognition,
256 there was only a weak correlation between SARS-CoV-2 memory T cells and individual
257 CCCoV strains (Figure 5H), which was in fact similar to other non-related common viral
258 antigens (Figure S5B). To further analyse the potential relevance of pre-existing immunity to
259 the anti-SARS-CoV-2 immune response, we re-stimulated expanded SARS-CoV-2-specific T
260 cell lines from COVID-19 patients and unexposed donors (Figure 5I, J). Only minimal and
261 highly variable cross-reactivity against CCCoV strains, but also against CMV or Influenza A
262 were detected in COVID-19 patients, as well as in expanded cells from unexposed individuals,
263 adding up to maximally 5% of the total response in individual donors (Figure 5I).

264 Taken together these data clearly argue against a strong protective effect of pre-existing
265 immunity in general and specifically against a major protective contribution of CCCoVs to the
266 T cell response against SARS-CoV-2 in unexposed donors, as well as in COVID-19 patients.

267

268 **Increased, but unfocussed and low affinity CD4+ T cell response against SARS-CoV-2** 269 **in severe disease**

270 Although we essentially excluded a general protective effect of pre-existing immunity we
271 demonstrated that cross-reactive memory T cells against SARS-CoV-2 antigens are common
272 in humans, increase with the immunological age and display rather low functional avidity. So
273 far, the consequences of this stochastic pre-existing memory are unclear. Since elderly suffer
274 more frequent from severe disease, we next compared the response of patients with mild
275 *versus* severe disease. Classification was based on WHO criteria, whereby WHO groups 3-5

276 (moderate) and 6-7 (severe) were combined to increase statistical power (see Table S1).
277 Interestingly, frequencies of reactive T cells against the single and pooled SARS-CoV-2
278 proteins, but not against Influenza A antigens positively correlated with disease severity
279 (Figure 6A). This was not due to an age bias in severe disease as shown for a selected group
280 of donors in the age range of 50-65 years (Figure 6B, C). Instead, we observed a clearly
281 increased immunological age of hospitalized *versus* non-hospitalized patients within the same
282 age group (Figure 6D).

283 To test whether the immunological age-related cross-reactive memory may impact on COVID-
284 19 severity, we also compared TCR avidities and clonalities of SARS-CoV-2-reactive T cells
285 from hospitalized *versus* non-hospitalized patients. Strikingly, SARS-CoV-2 reactive T cells
286 from hospitalized patients displayed significantly lower functional avidity compared to non-
287 hospitalized patients (Figure 6E-G). In line with this, SARS-CoV-2-specific T cells from
288 hospitalized COVID-19 patients displayed a trend towards a more diverse TCR repertoire
289 (Figure 6H) and reduced clonal expansions, as indicated by the lower Gini coefficient, as a
290 measure of the evenness of a population (Figure 6I). However, this was not significant due to
291 one outlier (grey dot in Figure 6G-I, see below). Thus despite strongly increased T cell
292 frequencies in severe COVID-19 (Figure 6A), this increase did not result from an expansion of
293 individual clones, but instead reflected a broad polyclonal response. We next analyzed the
294 distribution of the most clonally expanded TCRs per patient within the different clusters of the
295 single-cell RNA sequencing analysis. Interestingly, we observed a tendency that in mild
296 disease the most expanded clones were mainly restricted to the cytotoxic cluster, whereas in
297 more severe disease, they were scattered over several clusters (Figure 6J, K). One severe
298 COVID-19 patient (grey dot in Figure 6G-I) did not fit into this scheme and also showed a high
299 clonality strongly focused to the cytotoxic cluster (Figure 6K, lower right). Interestingly this
300 patient suffered from a CMV reactivation, which may account for expansion of cross-reactive
301 clones. Still the cells from this donor were of low avidity for SARS-CoV-2 antigens (Figure 6G,
302 grey dot) confirming the robustness of the avidity data.

303 In summary our data suggest that severe COVID-19 disease is characterized by a strong but
304 rather unfocused virus-specific CD4+ T cell response involving a broad polyclonal repertoire
305 of rather low avidity T cells. Such unfocused, low avidity response may in fact result from
306 preferential recruitment of a broad pre-existing memory repertoire preferentially present in the
307 elderly.

308 Discussion 309

310 Defining the parameters contributing to the high clinical variability of COVID-19 is essential to
311 predict disease outcome and develop effective therapeutic and vaccination strategies. Here
312 we provide two key observations, suggesting a negative impact of pre-existing T cell memory
313 which may explain the age-bias of COVID-19 severity: First, we show that all COVID-19
314 patients generate strong pro-inflammatory T cells responses, that increased with disease
315 severity. Unexpectedly, severe disease is associated with lower functional avidity and TCR
316 clonality. Second, we identify SARS-CoV-2 “pre-existing” T cell memory as a common feature
317 related to the immunological age of an individual, which recapitulates the low functional avidity
318 found in severe COVID-19 and suggests a causative relation.

319 Our cytometric and single-cell RNA sequencing characterization of SARS-CoV-2 memory T
320 cells confirmed previous results showing common characteristics of an anti-viral T cell
321 response but did not identify clear-cut differences between severe and mild disease.
322 Surprisingly, similar cell clusters were present in SARS-CoV-2-specific memory T cells from
323 unexposed controls. Thus quantitative differences rather than unique functionality profiles
324 develop in COVID-19. Indeed, all COVID-19 patients develop strong, pro-inflammatory Th1-
325 like CD4⁺ T cell responses directed against the three main proteins spike, membrane and
326 Ncap, as shown before for convalescent patients (Grifoni et al., 2020). Interestingly, despite
327 the reported T cell lymphopenia in severe disease, SARS-CoV-2-specific T cell frequencies
328 increased with disease severity (Anft et al., 2020; Peng et al., 2020). Compared to other
329 common viruses SARS-CoV-2-specific T cells showed signs of recent activation, such as
330 CD38, Ki-67 and PD1, as well as CD154 and high IL-21 production indicative of B cell helper
331 function. Also the slightly reduced expression of cytokines like IFN- γ , TNF- α and IL-2 compared
332 to other anti-viral responses may be related to the recent activation. Thus the T cell response
333 phenotype *per se* does not explain disease severity but will require detailed longitudinal
334 analysis in the future. The preferential formation of a highly focused clonal T cell population
335 within the cytotoxic cluster in mild COVID-19 suggests their potential protective function, which
336 may deserve further detailed analysis, including their peptide specificities.

337 We also characterized pre-existing memory as one factor for quantitative differences in the T
338 cell response in mild versus severe disease. The observation that SARS-CoV-2 specific T cells
339 were found in a subset of unexposed donors (Braun et al., 2020; Grifoni et al., 2020; Le Bert
340 et al., 2020; Mateus et al., 2020; Meckiff et al., 2020; Sekine et al., 2020; Weiskopf et al., 2020),
341 has initially fueled the hypothesis of protective pre-existing immunity, for example induced by
342 related CCCoVs preferentially in young people (Braun et al., 2020; Mateus et al., 2020). Such
343 heterologous immunity between related pathogens has been previously demonstrated mainly
344 in infection models (Welsh et al., 2010) but may also modulate human immune responses
345 (Bacher et al., 2019; Gras et al., 2010; Hayward et al., 2015; Koutsakos et al., 2019; Sridhar

346 et al., 2013). So far, cross-reactivity of SARS-CoV-2 reactive T cells was poorly characterized
347 and their functional impact remained unknown. In line with our results, a weak correlation
348 between CCCoV and SARS-CoV-2 T cell responses in unexposed donors has been identified
349 and cross-reactivity to CCCoV was observed in SARS-CoV-2-specific T cell lines directed
350 against the most homologous part of spike proteins (Braun et al., 2020) or selected
351 homologous peptides (Mateus et al., 2020). Our more detailed analysis of cross-reactivity in
352 healthy and COVID-19 patients argues against a major role of CCCoVs: Pre-existing memory
353 T cells were detected in all unexposed donors and their frequencies correlated with the
354 immunological age but not with CCCoV-specific memory. Furthermore pre-existing memory
355 cells displayed low functional avidity and were less focused on the dominant COVID-19 targets
356 spike, membrane and Ncap protein (Figure 1D) (Grifoni et al., 2020; Le Bert et al., 2020). Most
357 importantly, CCCoV cross-reactivity both within SARS-CoV-2-specific T cells from COVID-19
358 patients, as well as unexposed donors, was marginal despite the ubiquitous presence of a
359 strong CCCoV-specific memory T cell response in all tested donors. Interestingly, also Mateus
360 et al. found that SARS-CoV-2-specific, but not cross-reactive T cells against the homologous
361 CCCoV peptides increased in COVID-19 patients (Mateus et al., 2020), supporting our finding.
362 Thus CCCoV-specific T cell memory is common in the human population but seems to have
363 minimal impact on SARS-CoV-2-specific immunity. It is important to mention that our
364 demonstration of strong T cell memory against all four CCCoV strains in all tested donors may
365 be an encouraging sign that protective cellular immunity against SARS-CoV-2 might also
366 persist longterm, even if antibody responses are transient (Seow, 2020).

367 An even more important role of pre-existing memory in COVID-19 and for human immunity in
368 general is emerging from our analysis. In contrast to previous reports we find memory T cells
369 against SARS-CoV-2 in all tested unexposed donors. This probably reflects the high sensitivity
370 and specificity of the ARTE assay. In fact, lack of magnetic pre-selection, prolonged stimulation
371 times and the use of frozen PBMC may limit sensitivity and specificity (Bacher and Scheffold,
372 2013, 2015). However, this pre-existing memory does not represent classical heterologous
373 immunity between related pathogens. Instead, pre-existing SARS-CoV-2 memory has features
374 of an unbiased, stochastic cross-reactivity within a large TCR repertoire similar as observed
375 against other neoantigens. This is supported by its ubiquitous presence and broad protein
376 specificity (Figure 1D) as well as its strong positive correlation with total CD4+ memory (Figure
377 4D, E). Especially the low functional avidity argues against *in vivo* affinity selection (Figure 4G)
378 (Bacher et al., 2016). Memory T cells against neo-antigens are commonly detected in humans
379 (Bacher et al., 2013; Campion et al., 2014; Kwok et al., 2012; Su et al., 2013). This can be
380 explained by the known TCR-intrinsic cross-reactivity against related and even unrelated but
381 structurally similar peptides (Birnbaum et al., 2014; Sewell, 2012). Thus a highly diverse

382 memory pool, which accumulates in humans over lifetime contains TCRs specific for neo-
383 antigens similar to the naïve T cell pool.

384 The impact of pre-existing memory on T cell responses against neoantigens in humans is
385 poorly understood. However, its correlation with the immunological age suggests increasing
386 impact in the elderly (Lanzer et al., 2018; Lanzer et al., 2014; Woodland and Blackman, 2006)
387 and it is tempting to speculate that this may contribute to the increased risk for severe COVID-
388 19 in the aged population. Since memory T cells have a lower activation threshold, a large
389 number of suboptimal low avidity memory cells may compete and prevent naïve T cell
390 activation and high affinity selection (Lanzer et al., 2018). Indeed the size of the naïve T cell
391 pool has been shown to correspond to vaccination success (Kwok et al., 2012; Schulz et al.,
392 2015; Woodland and Blackman, 2006). Thus we hypothesize that pre-existing memory may
393 contribute to the reduced avidity and higher diversity of TCRs in severe COVID-19. Such a
394 polyclonal and low avidity T cell response may also be less susceptible to intrinsic negative
395 control mechanisms, which may explain the increased SARS-CoV-2-reactive T cell response.
396 Pre-existing memory indeed represents a general mechanism of immune-modulation towards
397 neo-antigens, especially in the elderly (Woodland and Blackman, 2006). Provided the great
398 heterogeneity within the human population with regard to antigen exposure and MHC
399 composition, we expect in fact highly variable and context-dependent effects of pre-existing
400 memory from protective to harmful. Therefore the impact of pre-existing memory on
401 neoantigen exposure, including sensitizing antigens, infections or vaccinations, as well as for
402 autoantigens has to be carefully evaluated in future studies.

403 **Acknowledgments**

404 We thank Chiara Romagnani and Ulf Klein for critical reading of the manuscript, the flow
405 cytometry facility Cyto Kiel, especially Esther Schiminsky and the Competence Centre for
406 Genomic Analysis (CCGA) Kiel, especially Janina Fuß, Sören Franzesburg, Yewgenia
407 Dolshanskaya, Catharina von der Lancken, Melanie Vollstedt and Melanie Schlapkohl for
408 support with cell sorting and single cell sequencing; the Clinical Trial Unit 2 of the University
409 Hospital of Cologne for help with recruiting study participants and technical assistance.

410

411 This research was supported by the German Research Foundation (DFG) under Germany's
412 Excellence Strategy - EXC 2167-390884018 Precision Medicine in Chronic Inflammation (to
413 P.B., A.F., A.S.); RU5042 – miTarget to P.B., A.F.; DFG grant n. 4096610003 to E.R; FL and
414 DE were supported by the E-Rare Joint Transnational research support (ERA-Net, LE3064/2-
415 1).

416

417

418 **Author contributions**

419 Conceptualization: P.B., A.S.; Investigation: P.B., E.R., G.R.M., C.S.; Formal analysis: P.B.,
420 E.R., D.E. P.K.; Resources: J.D., I.S., I.W., F.E., Y.K., M.J.G.T., C.C., F.T., P.R., R.M., K.P.W.,
421 F.L., J.R., M.K., O.A.C., P.K., A.F.; Funding acquisition: P.B., A.S.; All authors provided
422 discussion, participated in revising the manuscript, and agreed to the final version.

423

424

425 **Disclosure of potential conflicts of interest**

426 P.B., A.S. are consultants of Miltenyi Biotec, who own IP rights concerning parts of the ARTE
427 technology.

428 P.K. has received non-financial scientific grants from Miltenyi Biotec GmbH, Bergisch
429 Gladbach, Germany, and the Cologne Excellence Cluster on Cellular Stress Responses in
430 Aging-Associated Diseases, University of Cologne, Cologne, Germany, and received lecture
431 honoraria from or is advisor to Akademie für Infektionsmedizin e.V., Astellas Pharma, the
432 European Confederation of Medical Mycology, Gilead Sciences, GPR Academy
433 Ruesselsheim, MSD Sharp & Dohme GmbH, Noxxon N.V., and University Hospital, LMU
434 Munich outside the submitted work.

435 O.A.C. is supported by the German Federal Ministry of Research and Education, is funded by
436 the Deutsche Forschungsgemeinschaft (DFG, German Research Foundation) under
437 Germany's Excellence Strategy – CECAD, EXC 2030 – 390661388 and has received research
438 grants from, is an advisor to, or received lecture honoraria from Actelion, Allegra, Amplyx,
439 Astellas, Basilea, Biosys, Cidara, Da Volterra, Entasis, F2G, Gilead, Grupo Biotoscana, IQVIA,
440 Janssen, Matinas, Medicines Company, MedPace, Melinta, Menarini, Merck/MSD, Mylan,

441 Nabriva, Noxxon, Octapharma, Paratek, Pfizer, PSI, Roche Diagnostics, Scynexis, and
442 Shionogi.

443 FL is supported by German Ministry of Education and Research (01GM1908A) and E-Rare
444 Joint Transnational research support (ERA-Net, LE3064/2-1) and discloses speaker honoraria
445 from Grifols, Teva, Biogen, Bayer, Roche, Novartis, Fresenius, travel funding from Merck,
446 Grifols and Bayer and serving on advisory boards for Roche, Biogen and Alexion.

447 **References**

- 448 Anft, M., Paniskaki, K., Blazquez-Navarro, A., Atila, A., Doevelaar, N., Seibert, F., Hoelzer, B.,
449 Skrzypczyk, S., Kohut, E., Kurek, J., *et al.* (2020). COVID-19 progression is potentially driven
450 by T cell immunopathogenesis. medRxiv.
- 451 Bacher, P., Heinrich, F., Stervbo, U., Nienen, M., Vahldieck, M., Iwert, C., Vogt, K., Kollet, J.,
452 Babel, N., Sawitzki, B., *et al.* (2016). Regulatory T Cell Specificity Directs Tolerance versus
453 Allergy against Aeroantigens in Humans. *Cell* *167*, 1067-1078 e1016.
- 454 Bacher, P., Hohnstein, T., Beerbaum, E., Rocker, M., Blango, M.G., Kaufmann, S., Rohmel,
455 J., Eschenhagen, P., Grehn, C., Seidel, K., *et al.* (2019). Human Anti-fungal Th17 Immunity
456 and Pathology Rely on Cross-Reactivity against *Candida albicans*. *Cell* *176*, 1340-1355 e1315.
- 457 Bacher, P., and Scheffold, A. (2013). Flow-cytometric analysis of rare antigen-specific T cells.
458 *Cytometry A* *83*, 692-701.
- 459 Bacher, P., and Scheffold, A. (2015). New technologies for monitoring human antigen-specific
460 T cells and regulatory T cells by flow-cytometry. *Curr Opin Pharmacol* *23*, 17-24.
- 461 Bacher, P., Schink, C., Teutschbein, J., Kniemeyer, O., Assenmacher, M., Brakhage, A.A., and
462 Scheffold, A. (2013). Antigen-reactive T cell enrichment for direct, high-resolution analysis of
463 the human naive and memory Th cell repertoire. *J Immunol* *190*, 3967-3976.
- 464 Birnbaum, M.E., Mendoza, J.L., Sethi, D.K., Dong, S., Glanville, J., Dobbins, J., Ozkan, E.,
465 Davis, M.M., Wucherpfennig, K.W., and Garcia, K.C. (2014). Deconstructing the peptide-MHC
466 specificity of T cell recognition. *Cell* *157*, 1073-1087.
- 467 Braun, J., Loyal, L., Frentsch, M., Wendisch, D., Georg, P., Kurth, F., Hippenstiel, S.,
468 Dingeldey, M., Kruse, B., Fauchere, F., *et al.* (2020). SARS-CoV-2-reactive T cells in healthy
469 donors and patients with COVID-19. *Nature*.
- 470 Butler, A., Hoffman, P., Smibert, P., Papalex, E., and Satija, R. (2018). Integrating single-cell
471 transcriptomic data across different conditions, technologies, and species. *Nat Biotechnol* *36*,
472 411-420.
- 473 Campion, S.L., Brodie, T.M., Fischer, W., Korber, B.T., Rossetti, A., Goonetilleke, N.,
474 McMichael, A.J., and Sallusto, F. (2014). Proteome-wide analysis of HIV-specific naive and
475 memory CD4(+) T cells in unexposed blood donors. *J Exp Med* *211*, 1273-1280.
- 476 Diao, B., Wang, C., Tan, Y., Chen, X., Liu, Y., Ning, L., Chen, L., Li, M., Liu, Y., Wang, G., *et*
477 *al.* (2020). Reduction and Functional Exhaustion of T Cells in Patients With Coronavirus
478 Disease 2019 (COVID-19). *Front Immunol* *11*, 827.
- 479 Finak, G., McDavid, A., Yajima, M., Deng, J., Gersuk, V., Shalek, A.K., Slichter, C.K., Miller,
480 H.W., McElrath, M.J., Pric, M., *et al.* (2015). MAST: a flexible statistical framework for
481 assessing transcriptional changes and characterizing heterogeneity in single-cell RNA
482 sequencing data. *Genome Biol* *16*, 278.
- 483 Gras, S., Kedzierski, L., Valkenburg, S.A., Laurie, K., Liu, Y.C., Denholm, J.T., Richards, M.J.,
484 Rimmelzwaan, G.F., Kelso, A., Doherty, P.C., *et al.* (2010). Cross-reactive CD8+ T-cell
485 immunity between the pandemic H1N1-2009 and H1N1-1918 influenza A viruses. *Proc Natl*
486 *Acad Sci U S A* *107*, 12599-12604.
- 487 Greiling, T.M., Dehner, C., Chen, X., Hughes, K., Iniguez, A.J., Boccitto, M., Ruiz, D.Z.,
488 Renfro, S.C., Vieira, S.M., Ruff, W.E., *et al.* (2018). Commensal orthologs of the human
489 autoantigen Ro60 as triggers of autoimmunity in lupus. *Sci Transl Med* *10*.
- 490 Grifoni, A., Weiskopf, D., Ramirez, S.I., Mateus, J., Dan, J.M., Moderbacher, C.R., Rawlings,
491 S.A., Sutherland, A., Premkumar, L., Jadi, R.S., *et al.* (2020). Targets of T Cell Responses to
492 SARS-CoV-2 Coronavirus in Humans with COVID-19 Disease and Unexposed Individuals.
493 *Cell* *181*, 1489-1501 e1415.
- 494 Hayward, A.C., Wang, L., Goonetilleke, N., Fragaszy, E.B., Bermingham, A., Copas, A.,
495 Dukes, O., Millett, E.R., Nazareth, I., Nguyen-Van-Tam, J.S., *et al.* (2015). Natural T Cell-
496 mediated Protection against Seasonal and Pandemic Influenza. Results of the Flu Watch
497 Cohort Study. *Am J Respir Crit Care Med* *191*, 1422-1431.
- 498 Huang, C., Wang, Y., Li, X., Ren, L., Zhao, J., Hu, Y., Zhang, L., Fan, G., Xu, J., Gu, X., *et al.*
499 (2020). Clinical features of patients infected with 2019 novel coronavirus in Wuhan, China.
500 *Lancet* *395*, 497-506.

501 Korsunsky, I., Millard, N., Fan, J., Slowikowski, K., Zhang, F., Wei, K., Baglaenko, Y., Brenner,
502 M., Loh, P.R., and Raychaudhuri, S. (2019). Fast, sensitive and accurate integration of single-
503 cell data with Harmony. *Nat Methods* 16, 1289-1296.

504 Koutsakos, M., Illing, P.T., Nguyen, T.H.O., Mifsud, N.A., Crawford, J.C., Rizzetto, S., Eltahla,
505 A.A., Clemens, E.B., Sant, S., Chua, B.Y., *et al.* (2019). Human CD8(+) T cell cross-reactivity
506 across influenza A, B and C viruses. *Nat Immunol* 20, 613-625.

507 Kwok, W.W., Tan, V., Gillette, L., Littell, C.T., Soltis, M.A., LaFond, R.B., Yang, J., James,
508 E.A., and DeLong, J.H. (2012). Frequency of epitope-specific naive CD4(+) T cells correlates
509 with immunodominance in the human memory repertoire. *J Immunol* 188, 2537-2544.

510 Lanzer, K.G., Cookenham, T., Reiley, W.W., and Blackman, M.A. (2018). Virtual memory cells
511 make a major contribution to the response of aged influenza-naive mice to influenza virus
512 infection. *Immun Ageing* 15, 17.

513 Lanzer, K.G., Johnson, L.L., Woodland, D.L., and Blackman, M.A. (2014). Impact of ageing on
514 the response and repertoire of influenza virus-specific CD4 T cells. *Immun Ageing* 11, 9.

515 Le Bert, N., Tan, A.T., Kunasegaran, K., Tham, C.Y.L., Hafezi, M., Chia, A., Chng, M.H.Y., Lin,
516 M., Tan, N., Linster, M., *et al.* (2020). SARS-CoV-2-specific T cell immunity in cases of COVID-
517 19 and SARS, and uninfected controls. *Nature*.

518 Mateus, J., Grifoni, A., Tarke, A., Sidney, J., Ramirez, S.I., Dan, J.M., Burger, Z.C., Rawlings,
519 S.A., Smith, D.M., Phillips, E., *et al.* (2020). Selective and cross-reactive SARS-CoV-2 T cell
520 epitopes in unexposed humans. *Science*.

521 Meckiff, B.J., Ramirez-Suastegui, C., Fajardo, V., Chee, S.J., Kusnadi, A., Simon, H., Grifoni,
522 A., Pelosi, E., Weiskopf, D., Sette, A., *et al.* (2020). Single-cell transcriptomic analysis of
523 SARS-CoV-2 reactive CD4 (+) T cells. *bioRxiv*.

524 Peng, Y., Mentzer, A.J., Liu, G., Yao, X., Yin, Z., Dong, D., Dejnirattisai, W., Rostron, T.,
525 Supasa, P., Liu, C., *et al.* (2020). Broad and strong memory CD4 (+) and CD8 (+) T cells
526 induced by SARS-CoV-2 in UK convalescent COVID-19 patients. *bioRxiv*.

527 Schulz, A.R., Malzer, J.N., Domingo, C., Jurchott, K., Grutzkau, A., Babel, N., Nienen, M.,
528 Jelinek, T., Niedrig, M., and Thiel, A. (2015). Low Thymic Activity and Dendritic Cell Numbers
529 Are Associated with the Immune Response to Primary Viral Infection in Elderly Humans. *J*
530 *Immunol* 195, 4699-4711.

531 Sekine, T., Perez-Potti, A., Rivera-Ballesteros, O., Strålin, K., Gorin, J.B., Olsson, A.,
532 Llewellyn-Lacey, S., Kamal, H., Bogdanovic, G., Muschiol, S., *et al.* (2020). Robust T cell
533 immunity in convalescent individuals with asymptomatic or mild COVID-19. *bioRxiv*.

534 Seow, J. (2020). Longitudinal evaluation and decline of antibody responses in SARS-CoV-2
535 infection. *medRxiv*.

536 Sette, A., and Crotty, S. (2020). Pre-existing immunity to SARS-CoV-2: the knowns and
537 unknowns. *Nat Rev Immunol*.

538 Sewell, A.K. (2012). Why must T cells be cross-reactive? *Nat Rev Immunol* 12, 669-677.

539 Sridhar, S., Begom, S., Bermingham, A., Hoschler, K., Adamson, W., Carman, W., Bean, T.,
540 Barclay, W., Deeks, J.J., and Lalvani, A. (2013). Cellular immune correlates of protection
541 against symptomatic pandemic influenza. *Nat Med* 19, 1305-1312.

542 Su, L.F., Kidd, B.A., Han, A., Kotzin, J.J., and Davis, M.M. (2013). Virus-specific CD4(+)
543 memory-phenotype T cells are abundant in unexposed adults. *Immunity* 38, 373-383.

544 Tan, L., Wang, Q., Zhang, D., Ding, J., Huang, Q., Tang, Y.Q., Wang, Q., and Miao, H. (2020).
545 Lymphopenia predicts disease severity of COVID-19: a descriptive and predictive study. *Signal*
546 *Transduct Target Ther* 5, 33.

547 Wang, D., Hu, B., Hu, C., Zhu, F., Liu, X., Zhang, J., Wang, B., Xiang, H., Cheng, Z., Xiong,
548 Y., *et al.* (2020). Clinical Characteristics of 138 Hospitalized Patients With 2019 Novel
549 Coronavirus-Infected Pneumonia in Wuhan, China. *JAMA*.

550 Weiskopf, D., Schmitz, K.S., Raadsen, M.P., Grifoni, A., Okba, N.M.A., Endeman, H., van den
551 Akker, J.P.C., Molenkamp, R., Koopmans, M.P.G., van Gorp, E.C.M., *et al.* (2020). Phenotype
552 and kinetics of SARS-CoV-2-specific T cells in COVID-19 patients with acute respiratory
553 distress syndrome. *Sci Immunol* 5.

554 Welsh, R.M., Che, J.W., Brehm, M.A., and Selin, L.K. (2010). Heterologous immunity between
555 viruses. *Immunol Rev* 235, 244-266.

556 Wilk, A.J., Rustagi, A., Zhao, N.Q., Roque, J., Martinez-Colon, G.J., McKechnie, J.L., Ivison,
557 G.T., Ranganath, T., Vergara, R., Hollis, T., *et al.* (2020). A single-cell atlas of the peripheral
558 immune response in patients with severe COVID-19. *Nat Med* 26, 1070-1076.
559 Woodland, D.L., and Blackman, M.A. (2006). Immunity and age: living in the past? *Trends*
560 *Immunol* 27, 303-307.
561 Yang, X., Yu, Y., Xu, J., Shu, H., Xia, J., Liu, H., Wu, Y., Zhang, L., Yu, Z., Fang, M., *et al.*
562 (2020). Clinical course and outcomes of critically ill patients with SARS-CoV-2 pneumonia in
563 Wuhan, China: a single-centered, retrospective, observational study. *Lancet Respir Med* 8,
564 475-481.
565 Zheng, H.Y., Zhang, M., Yang, C.X., Zhang, N., Wang, X.C., Yang, X.P., Dong, X.Q., and
566 Zheng, Y.T. (2020). Elevated exhaustion levels and reduced functional diversity of T cells in
567 peripheral blood may predict severe progression in COVID-19 patients. *Cell Mol Immunol* 17,
568 541-543.
569

570 **Figure Legends**

571

572 **Figure 1. Identification of immunogenic SARS-CoV-2 proteins**

573 (A) Frequencies of reactive CD154+CD45RA- memory CD4+ T cells (T_{mem}) against individual
574 SARS-CoV-2 proteins in unexposed donors (n=9) and COVID-19 patients (n=11; non-
575 hospitalized n=8; hospitalized n=3).

576 (B) Representative dot plot examples for *ex vivo* detection of SARS-CoV-2-reactive CD4+ T
577 cells by ARTE. Absolute cell counts after magnetic CD154+ enrichment from 1x10⁷ PBMCs
578 are indicated.

579 (C) Frequencies of SARS-CoV-2-reactive T_{mem} against individual or pooled spike,
580 membrane, Ncap proteins or a pool of Influenza A proteins (containing HA, MP1, MP2, NP and
581 NA). Unexposed donors (n=50), COVID-19 patients (n=49).

582 (D) Proportion of SARS-CoV-2 proteins recognized by CD4+ T cells in unexposed donors (n=9)
583 and COVID-19 patients (n=11).

584 Each symbol in (A, C) represents one donor. (A) Box-and-whisker plots display quartiles and
585 range. (C) Horizontal lines indicate geometric mean. Statistical differences: (C) Two-tailed
586 Mann-Whitney test.

587

588

589 **Figure 2. Inflammatory SARS-CoV-2-specific CD4+ T cell responses in COVID-19** 590 **patients**

591 (A) *Ex vivo* Ki-67 and CD38 expression of SARS-CoV-2 pool-reactive CD154+ T_{mem}.
592 Unexposed donors (n=50), COVID-19 patients (n=49).

593 (B) *Ex vivo* Ki-67 and CD38 staining of SARS-CoV-2 pool- or Influenza A-reactive CD154+
594 T_{mem} from COVID-19 patients at different time points after disease onset. Percentage of Ki-
595 67+ and/ or CD38+ cells within CD154+ T_{mem} are indicated.

596 (C) Spearman correlation of Ki-67 and CD38 expression or frequencies of SARS-CoV-2 pool-
597 reactive CD154+ T_{mem} and days since disease onset in COVID-19 patients (n=49).

598 (D) *Ex vivo* cytokine and phenotype staining of SARS-CoV-2 pool-reactive CD154+ T_{mem}
599 from a COVID-19 patient. Percentage of marker positive cells within CD154+ T_{mem} are
600 indicated.

601 (E) *Ex vivo* cytokine production and phenotype of SARS-CoV-2 pool-reactive cells. Upper row:
602 within CD154+ T_{mem} and lower row: within total CD4+ T cells. Unexposed donors (n=50; IL-
603 21 n=31), COVID-19 patients (n=49; IL-21 n=26).

604 (F) Heatmap depicting *ex vivo* cytokine production of virus-reactive memory T cells (n=26-50).
605 Cytokine production within CD154+ T_{mem} was measured by flow cytometry and mean values
606 were Z score normalized for each cytokine.

607 Each symbol in (A, C, E) represents one donor, horizontal lines indicate (A) geometric mean,
608 (E) mean. Statistical differences: (A, E) Two-tailed Mann-Whitney test.

609

610

611 **Figure 3. Single cell RNA sequencing of SARS-CoV-2-reactive CD4+ T cells**

612 (A) Single cell gene expression of FACS purified *ex vivo* isolated CD154+ memory T cells
613 following stimulation with pooled SARS-CoV-2 spike, membrane and Ncap proteins from
614 unexposed donors (n=6) and COVID-19 patients (n=14). UMAP visualization of the subset
615 composition of SARS-CoV-2 reactive CD4+ T cells colored by functional gene expression
616 clusters.

617 (B) Dot plot visualization showing the expression of selected marker genes in each SARS-
618 CoV-2 T cell cluster. Colors represent the Z-score normalized expression levels and size
619 indicates the proportion of cells expressing the respective genes.

620 (C) Proportion of cells falling within each cluster for the individual donors (unexposed donors
621 n=6; non-hospitalized COVID-19 patients n=6; hospitalized COVID-19 patients (n=8).

622 Each symbol in (C) represents one donor, horizontal lines indicate mean.

623

624

625 **Figure 4. SARS-CoV-2 reactive CD4+ T cells in healthy donors**

626 (A) CD45RA and CCR7 staining of SARS-CoV-2- or Influenza A-reactive CD154+ cells in
627 unexposed donors or COVID-19 patients. Percentage of marker positive cells within CD154+
628 is indicated.
629 (B) Proportion of memory cells within SARS-CoV-2 reactive cells in unexposed donors (n=50)
630 or COVID-19 patients (n=49).
631 (C, D) Spearman correlation between the frequencies of SARS-CoV-2 pool-reactive T cells in
632 unexposed donors and (C) the age of donors or (D) the proportion of memory cells within the
633 total CD4+ population, corresponding to the immunological age.
634 (E) Pearson correlation between the proportion of memory cells within the antigen-specific T
635 cells (y-axis) and the proportion of memory cells within the total CD4+ population (x-axis;
636 immunological age) is shown for exposed and unexposed donors for SARS-CoV-2 and CMV.
637 (F, G) SARS-CoV-2 pool-reactive CD154+ Tmem from unexposed donors and COVID-19
638 patients were FACS purified, expanded and re-stimulated with decreasing antigen
639 concentration in the presence of autologous antigen-presenting cells. (F) CD154 or TNF- α
640 expression for the indicated concentration per peptide. (G) EC50 values were calculated from
641 dose-response curves. Left: SARS-CoV-2 reactive cells from unexposed donors n=8, COVID-
642 19 patients n=19; right: CMV-reactive cells n=5 or SARS-CoV-2 reactive from COVID-19
643 patients (n=19).
644 Each symbol in (B, C, D, E, G) represents one donor, horizontal lines indicate (B) mean. (G)
645 Box-and-whisker plots display quartiles and range. Statistical differences: (G) Two-tailed
646 Mann-Whitney test.

647
648

649 **Figure 5. Human CD4+ T cell response against common cold viruses (CCCoVs)**

650 (A) *Ex vivo* detection of reactive CD4+ T cells against CCCoV spike proteins by ARTE.
651 Absolute cell counts after magnetic CD154+ enrichment from 1×10^7 PBMCs are indicated.
652 (B) Summary of CCCoV-reactive Tmem frequencies in healthy donors (n=34).
653 (C) CD45RA and CCR7 staining of CCCoV-reactive CD154+ cells in healthy donors.
654 Percentage of marker positive cells within CD154+ is indicated.
655 (D) Proportion of memory cells within CCCoV-reactive cells in healthy donors (n=34).
656 (E-G) CD154+ Tmem reactive against a pool of the 229E, OC43, HKU1 and NL63 spike
657 proteins or reactive against the SARS-CoV-2 spike, membrane and Ncap proteins were FACS
658 purified, expanded and re-stimulated. (E) Cells were re-stimulated with decreasing antigen
659 concentration. EC50 values were calculated from dose-response curves. (F) Reactivity of the
660 expanded cell lines against CCCoV spike pool or SARS-CoV-2 spike protein, respectively
661 (n=3-4). (G) Representative dot plots for re-stimulation. Percentage of CD154+TNF α + cells
662 within CD4+ is indicated.
663 (H) Spearman correlation between CD154+ Tmem frequencies reactive against different
664 CCCoVs or CCCoVs and SARS-CoV-2 spike (n=34).
665 (I, J) Expanded SARS-CoV-2 pool-reactive T cells from COVID-19 patients (n=19) or
666 unexposed individuals (n=9) were re-stimulated with different antigens in presence of
667 autologous antigen-presenting cells. (I) Signal:noise ratio of stimulated *versus* non-stimulated
668 control. A detection limit (dashed line), was defined as signal:noise ratio ≥ 3 . (J) Dot plot
669 examples for re-stimulation of a COVID-19 patient. Cells were gated on CD4+ T cells and
670 percentages of CD154+TNF α + cells are indicated.
671 Each symbol in (B, D, E, F, H, I) represents one donor, horizontal lines indicate (A, B) mean,
672 (I) geometric mean. (E-F) Box-and-whisker plots display quartiles and range. Statistical
673 differences: (B, D) Friedman test with Dunn's post hoc test, (E) Two-tailed Mann-Whitney test.

674
675

676 **Figure 6. Unfocussed T cell response in severe COVID-19**

677 (A) Frequencies of SARS-CoV-2-reactive Tmem. The highest COVID-19 severity level during
678 disease was assessed based on WHO criteria, whereby WHO groups 3-5 (moderate) and 6-7
679 (severe) were combined to increase statistical power (see Table S1). Unexposed donors n=50,
680 Non-hospitalized n=26 (WHO 1-2), mild-moderate n=12 (WHO 3 n=2, WHO 4 n=6, WHO 5

681 n=4), severe n=11 (WHO 6 n=5, WHO 7 n=6); patients with active disease at the time point of
682 sampling are indicated with a square.
683 (B) Age distribution within the different disease groups and controls and within the age-
684 selected donors from 50-65 years.
685 (C) Frequencies of SARS-CoV-2-pool-reactive Tmem in age-selected donors.
686 (D) Immunological age of the age-selected donors, indicated as the proportion of memory cells
687 within the total CD4+ population.
688 (E-G) SARS-CoV-2 pool-reactive CD154+ Tmem were FACS purified, expanded and re-
689 stimulated with decreasing antigen concentration in the presence of autologous antigen-
690 presenting cells. (E) CD154 or TNF- α expression for the indicated concentration per peptide.
691 (G) Dose-response curves of expanded T cell lines, restimulated with decreasing antigen
692 concentrations. (F) EC50 values were calculated from dose-response curves. Non-
693 hospitalized n=13, hospitalized n=6.
694 (H, I) T cell receptor (TCR) sequence analysis from single cell data of the top 50 expanded
695 clonotypes. (H) Simpson Index of TCR diversity. (I) Gini coefficient depicting the distribution of
696 TCR sequences (0 is total equality, i.e. all clones have the same proportion, 1 total inequality,
697 i.e. a population dominated by a single clone). Non-hospitalized n=6, hospitalized n=8.
698 (J) Representative distribution of the top 3 expanded TCR clonotypes projected to the UMAP
699 analysis for one exemplary non-hospitalized and one hospitalized COVID-19 patient.
700 (K) Proportional distribution of the top 3 expanded clonotypes on the different Seurat clusters
701 for each analyzed patient (non-hospitalized n=6; hospitalized n=8).
702 Each symbol in (A-D, G-I) represents one donor, horizontal lines indicate (A-D) mean. (G-I)
703 Box-and-whisker plots display quartiles and range. Statistical differences: (A) Kruskal-Wallis
704 test with Dunn's post hoc test, significant differences are indicated. (G-I) Two-tailed Mann-
705 Whitney test.

706
707

708 **Figure S1. Detection of SARS-CoV-2 reactive CD4+ T cells by ARTE**

709 (A) *Ex vivo* detection of SARS-CoV-2 pool-reactive CD4+ T cells by ARTE. Percentage within
710 CD4+ T cells and absolute cell counts before and after magnetic CD154+ enrichment from
711 1×10^7 PBMCs are indicated.
712 (B and C) Re-stimulation of FACS purified, expanded SARS-CoV-2 pool-reactive CD154+ T
713 cells with the SARS-CoV-2 pool or Tetanus as control antigen. (B) Percentage of
714 CD154+TNF α + cells within CD4+ is indicated. (C) Statistical summary, each symbol
715 represents one donor. Box-and-whisker plots display quartiles and range. Unexposed donors
716 (n=9), COVID-19 patients (n=19).

717
718

719 **Figure S2. Pattern of SARS-CoV-2 reactive CD4+ T cells compared to other anti-viral responses.**

720
721 (A) Spearman correlation of cytokine and phenotypic marker expression of SARS-CoV-2 pool-
722 reactive CD154+ Tmem and days since disease onset.
723 (B) *Ex vivo* cytokine production and phenotype of SARS-CoV-2-reactive cells of
724 reconvalescent COVID-19 patients in comparison to other anti-viral responses in SARS-CoV-
725 2 unexposed donors (n=26-50).
726 Each symbol in (A, B) represents one donor.

727
728

729 **Figure S3. Gene expression of SARS-CoV-2 reactive CD4+ T cell clusters**

730 Single cell transcriptomes of FACS purified *ex vivo* isolated CD154+ memory T cells following
731 stimulation with pooled SARS-CoV-2 spike, membrane and Ncap proteins from unexposed
732 donors (n=6) and COVID-19 patients (n=14).
733 (A) Heatmap depicting Z-score normalized expression levels of the top 10 differential
734 expressed marker genes of each cluster and other selected genes.

735 (B) UMAP visualization of the subset composition of SARS-CoV-2 reactive CD4+ T cells
736 colored by functional gene expression clusters for unexposed donors (n=6) and non-
737 hospitalized (n=6), moderate (WHO 4-5; n=5) and severe (WHO 6-7; n=3) COVID-19 patients.
738

739
740 **Figure S4. Proportion of neoantigen-specific memory T cells correlates with the**
741 **immunological age.**

742 Pearson correlation between the proportion of memory cells within the antigen-specific T cells
743 (y-axis) and the proportion of memory cells within the total CD4+ population is shown for the
744 neoantigen keyhole limpet hemocyanin (KLH).
745

746
747 **Figure S5. Correlations of SARS-CoV-2-reactive T cells of unexposed donors with the**
748 **response against other common viruses**

749 (A) Pearson correlation between the proportion of memory cells within the CCCoV spike-
750 specific T cells (y-axis) and the proportion of memory cells within the total CD4+ population (x-
751 axis, immunological age) in SARS-CoV2-unexposed donors.

752 (B) Spearman correlation between CD154+ Tmem frequencies reactive against different
753 CCCoVs or SARS-CoV-2 and Influenza A (H1N1), Cytomegalovirus (CMV), Epstein-Barr
754 Virus (EBV), Adenovirus (AdV) or tetanus in unexposed donors.

755 Each symbol in (A, B) represents one donor.
756

757
758 **Figure S6. SARS-CoV-2-reactive T cell in age-selected donors.**

759 (A) Frequencies of Tmem reactive against the indicated SARS-CoV-2 proteins in donors with
760 an age range of 50-65. The highest COVID-19 severity level during disease was assessed
761 based on WHO criteria, whereby WHO groups 3-5 (moderate) and 6-7 (severe) were combined
762 to increase statistical power (see table S1). Unexposed donors n=14, Non-hospitalized n=7
763 (WHO 1-2), moderate n=7 (WHO 3 n=1, WHO 4 n=3, WHO 5 n=3), severe n=5 (WHO 6 n=2,
764 WHO 7 n=3,). Each symbol in represents one donor, horizontal lines indicate mean.

765 **Materials & Methods**

766

767 CONTACT FOR REAGENT AND RESOURCE SHARING

768

769 Further information and requests for reagents may be directed to the corresponding author
770 Petra Bacher (petra.bacher@ikmb.uni-kiel.de).

771

772 EXPERIMENTAL MODEL AND SUBJECT DETAILS

773

774 **COVID-19 patients and unexposed donors**

775 This study was approved by the Institutional Review board of the UKSH Kiel (Identifier D
776 474/20), the University Hospital Frankfurt (Identifier 11/17) and patients were enrolled in the
777 protocol Coronavirus Disease 19 – BioMaSOTA - Genetic factors and longitudinal monitoring
778 of the immune response in COVID-19 (Identifier of the University of Cologne Ethics Committee
779 20-1295) and Improving Diagnosis of Severe Infections of Immunocompromised Patients
780 (Identifier of the University of Cologne Ethics Committee 08-160) and signed informed
781 consents.

782 Peripheral EDTA blood samples were collected between April and July 2020 from 49 COVID-
783 19 patients and from 50 in-house volunteers as unexposed controls (Table S1). 44 of 49
784 COVID-19 patients were tested positive and for SARS-CoV-2 RNA. We included 5 mild cases
785 of COVID-19 without positive SARS-CoV2 RNA test, but with positive detection of antibodies
786 using a certified antibody test (Elecsys Anti-SARS-CoV-2, Roche Diagnostics GmbH,
787 Mannheim, Germany) who had clinical symptoms suggestive of COVID-19 and a traceable
788 contact person found positive.

789 All, except three active COVID-19 patients who had a positive SARS-CoV-2 RNA test, were
790 tested positive for SARS-CoV-2 antibodies (Elecsys Anti-SARS-CoV-2, Roche Diagnostics
791 GmbH and/ or Anti-SARS-CoV-2 ELISA, Euroimmun, Lübeck, Germany). All healthy controls
792 were tested negative for SARS-CoV-2 antibodies (Elecsys Anti-SARS-CoV-2, Roche
793 Diagnostics GmbH). The highest COVID-19 severity was assessed based on WHO ordinal
794 scale (<https://www.who.int/publications/i/item/covid-19-therapeutic-trial-synopsis>).

795

796 METHOD DETAILS

797

798 **Antigens**

799 Pools of lyophilized 15-mer peptides with 11-amino acid overlap, covering the complete
800 protein sequence were purchased from Miltenyi Biotec (Bergisch Gladbach, Germany): SARS-

801 CoV-2 Membrane, Ncap or JPT (Berlin, Germany): SARS-CoV-2 Spike N-term, Spike C-term,
802 AP3A, ORF9B, ORF10, NS6, NS7a, NS7b, NS8, VEMP, Y14.

803 Peptide pools of control antigens Influenza A H1N1 (HA, MP1, MP2, NP and NA), CMV (pp65,
804 IE-1), EBV (EBNA1, BZLF1, LMP2A, LMP1), AdV (Hexon) were purchased from Miltenyi
805 Biotec and CCCoV Spike proteins (229E, OC43, HKU1, NL63) from JPT. Pools were
806 resuspended according to manufacturer's instructions and cells were stimulated at a
807 concentration of 0.5 µg/peptide/ml. Tetanus-toxoid was purchased from Statens Serum
808 Institute and used at a concentration of 10µg/ml.

809

810 **Antigen-reactive T cell enrichment (ARTE)**

811 Peripheral blood mononuclear cells were freshly isolated from 20-50ml EDTA blood on the day
812 of blood donation by density gradient centrifugation (Biocoll; Biochrom, Berlin, Germany).
813 Antigen-reactive T cell enrichment (ARTE) was performed as previously described (Bacher et
814 al., 2019; Bacher et al., 2016). In brief, 0.5-2×10⁷ PBMCs were plated in RPMI-1640 medium
815 (GIBCO), supplemented with 5% (v/v) human AB-serum (Sigma Aldrich, Schnelldorf,
816 Germany) at a cell density of 1×10⁷ PBMCs / 2 cm² in cell culture plates and stimulated for
817 7 hr in presence of 1 µg/ml CD40 and 1 µg/ml CD28 pure antibody (both Miltenyi Biotec,
818 Bergisch Gladbach, Germany). 1 µg/ml Brefeldin A (Sigma Aldrich) was added for the last 2
819 hr.

820 Cells were labeled with CD154-Biotin followed by anti-Biotin (CD154 MicroBead Kit, Miltenyi
821 Biotec) and magnetically enriched by two sequential MS columns (Miltenyi Biotec). Surface
822 staining was performed on the first column, followed by fixation and intracellular staining on
823 the second column. Frequencies of antigen-specific T cells were determined based on the cell
824 count of CD154+ T cells after enrichment, normalized to the total number of CD4+ T cells
825 applied on the column. For each stimulation, CD154+ background cells enriched from the non-
826 stimulated control were subtracted.

827

828 **Flow cytometry**

829 Cells were stained in different combinations of fluorochrome-conjugated antibodies (see Key
830 Resources Table). Viability 405/520 Fixable Dye (Miltenyi Biotec) was used to exclude dead
831 cells. For intracellular staining cells were fixed and permeabilized with the Inside stain Kit
832 (Miltenyi Biotec). Data were acquired on a or LSR Fortessa (BD Bioscience, San Jose, CA,
833 USA). Screening of expanded T cell lines on 384-well plates was performed on a
834 MACSQuantX Analyzer (Miltenyi Biotec). FlowJo (Treestar, Ashland, OR, USA) software was
835 used for analysis.

836

837 ***In vitro* expansion and re-stimulation of antigen-reactive T cell lines**

838 For expansion of antigen-specific T cell lines, PBMCs were stimulated for 6 hr, CD154+ cells
839 were isolated by MACS and further purified by FACS sorting on a FACS Aria Fusion (BD
840 Bioscience, San Jose, CA, USA) based on dual expression of CD154 and CD69. Purified
841 CD154+ T cells were expanded in presence of 1:100 autologous antigen-loaded irradiated
842 feeder cells in TexMACS medium (Miltenyi Biotec), supplemented with 5% (v/v) human AB-
843 serum (GemCell), 200 U/ml IL-2 (Proleukin; Novartis, Nürnberg, Germany), and 100 IU/ml
844 penicillin, 100 µg/ml streptomycin, 0.25 µg/ml amphotericin B (Antibiotic Antimycotic Solution,
845 Sigma Aldrich) at a density of 2.5×10^6 cells/cm². During expansion for 2-3 weeks, medium
846 was replenished and cells were split as needed.

847 For re-stimulation, fastDCs were generated from autologous CD14+ MACS isolated
848 monocytes (CD14 MicroBeads; Miltenyi Biotec) by cultivation in X-Vivo™15 medium
849 (BioWhittaker/Lonza), supplemented with 1000 IU/ml GM-CSF and 400 IU/ml IL-4 (both
850 Miltenyi Biotec). Before re-stimulation expanded T cells were rested in RPMI-1640 + 5 %
851 human AB-serum without IL-2 for 2 days. $0.5-1 \times 10^5$ expanded T cells were plated with
852 fastDCs in a ratio 1:1 of in 384-well flat bottom plates and re-stimulated for 6 h, with 1 µg/ml
853 Brefeldin A (Sigma Aldrich) added for the last 4 hr.

854

855 **Cell isolation and single-cell RNA-seq assay (10x Genomics)**

856 For single cell transcriptomics, CD154+ cells were isolated by MACS and further purified by
857 FACS sorting on a MACSQuant Tyto (Miltenyi Biotec) based on dual expression of CD154 and
858 CD69. Sorted CD154+ T cells were removed from the sorting chamber into pre-coated low-
859 bind collection tubes, 1ml RPMI1640 medium supplemented with 5% AB Serum was added,
860 and cells were centrifuged for 5 min at 400 x g, 4°C. The supernatant was carefully removed
861 leaving 10-30µl to reach a maximum concentration of 1000 cells /µl.

862 Single-cell suspensions were loaded on a Chromium Chip G (10x Genomics) according to the
863 manufacturer's instructions for processing with the Chromium Next GEM Single Cell 5' Library
864 and Gel Bead Kit v1.1. Depending on the number of cells available for each patient, a
865 maximum of 30,000 cells were loaded for each reaction. TCR single-cell libraries were
866 subsequently prepared from the same cells with the Chromium Single Cell V(D)J Enrichment
867 Kit, Human T Cell. Libraries were sequenced on Illumina NovaSeq 6000 machine with 2x100
868 bp for gene expression, aiming for 50,000 reads per cell and 2x150 bp and 5000 reads per cell
869 for TCR libraries.

870

871 **Single cell T cell receptor (TCR) sequence analysis**

872 Single-cell T-cell receptor repertoire clonotype tables were generated using the VDJ command
873 of the Cellranger software, version 3.1.0. from 10xGenomics and using the reference GRCh38
874 version 2.0.0. Clonotype tables were filtered in order to include only cells which passed quality

875 filtering in the gene expression analysis. In addition, clonotypes were stringently filtered for
876 possible doublets by removing clonotypes (i) found in 1 cell only and containing more than 1
877 TCR alpha and 1 TCR beta (ii) containing more than 1 TCR alpha and no TCR beta sequence
878 (iii) containing more than 1 TCR beta and no TCR alpha sequence (iv) containing more than 2
879 TCR alpha or more than 2 TCR beta sequences.

880 Alpha diversity measures were calculated for each patient either for the whole repertoire or
881 divided based on Seurat clusters. R packages “vegan” and “tcR” were used to calculate the
882 Inverse Simpson diversity index and the Gini inequality index, respectively. For these analyses
883 samples were normalized by selection of the most abundant 50 clonotypes in order to remove
884 the impact of different sample sizes (number of cells per sample) and to analyze only the
885 distribution of the most expanded clonotypes.

886 Analysis of the most expanded clonotypes was conducted by selecting the 3 most expanded
887 clonotypes per sample. To evaluate potentially existing preferential cumulation of most
888 expanded clonotypes in certain functional clusters, the proportion of cells carrying these
889 clonotypes falling in each distinct Seurat cluster was calculated.

890

891 **Single-cell transcriptome analysis**

892 The preprocessing of the scRNA-data was performed with the 10x Genomics' Cell Ranger
893 software v3.1.0 using the reference GRCh38 v3.0.0 for the mappings. The resulting filtered
894 feature-barcode matrix files were analyzed with the R package Seurat v.3.2.0 (Butler et al.,
895 2018). Thereby, all genes with a detected expression in less than 0.1% of the non-empty cells
896 were excluded. Moreover, TCR genes were not considered for further analyses to avoid
897 functional clustering of cells based on TCR information. To minimize the number of doublets,
898 empty cells, and cells with a transcriptome in low quality, only cells harboring between 840
899 (minimum median among samples) and 3000 RNA features and less than 5% mitochondrial
900 RNA were selected for further processing. Afterwards, data were log-normalized and scaled
901 based on all genes. After performing a PCA dimensionality reduction (20 dimensions) with the
902 RunPCA function, the expression values were corrected for effects caused by different sample
903 preparation time points in time using the R package Harmony v1.0 (Korsunsky et al., 2019). In
904 the final steps, the Uniform Manifold Approximation and Projection (UMAP) dimensional
905 reduction was performed with the RunUMAP function using 20 dimensions, a shared nearest
906 neighbor graph was created with the FindNeighbors method, and the clusters identification
907 was performed with a resolution of 0.2 using the FindClusters function. Positive cluster marker
908 genes were determined using FindMarkers with the MAST method (Finak et al., 2015).
909 Thereby, only genes with detected expression in at least 25% of the cells in the respective
910 cluster were considered.

911

912 **QUANTIFICATION AND STATISTICAL ANALYSIS**

913 Statistical parameters including the exact value of n, the definition of center, dispersion and
914 precision measure, and statistical significance are reported in the Figures and the Figure
915 Legends. Statistical tests were performed with GraphPad PRISM software 8.4 (GraphPad
916 Software, La Jolla, CA, USA). Statistical tests were selected based on appropriate
917 assumptions with respect to data distribution and variance characteristics, p values < 0.05
918 were considered statistically significant.

919

920 **DATA AND SOFTWARE AVAILABILITY**

921

922 **Software**

923 Flow-cytometry data were analyzed using FlowJo (Treestar, Ashland, OR, USA) software.
924 Graphics and statistics were created with GraphPad PRISM software version 8.4.3. (GraphPad
925 Software, La Jolla, CA, USA). Heatmaps were generated using Genesis software (Sturn et al.,
926 2002), version 1.7.7.

Figure 1

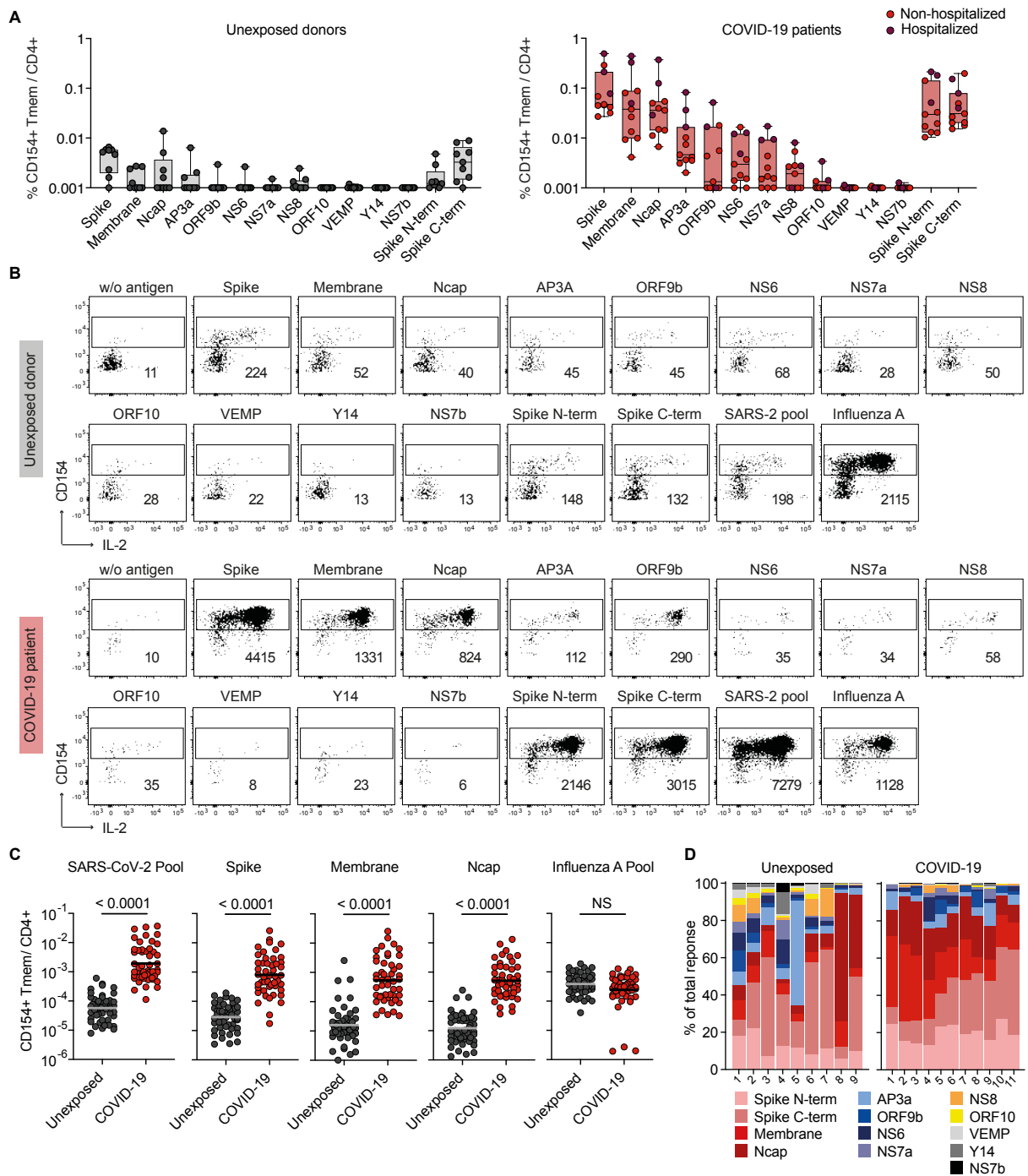


Figure 2

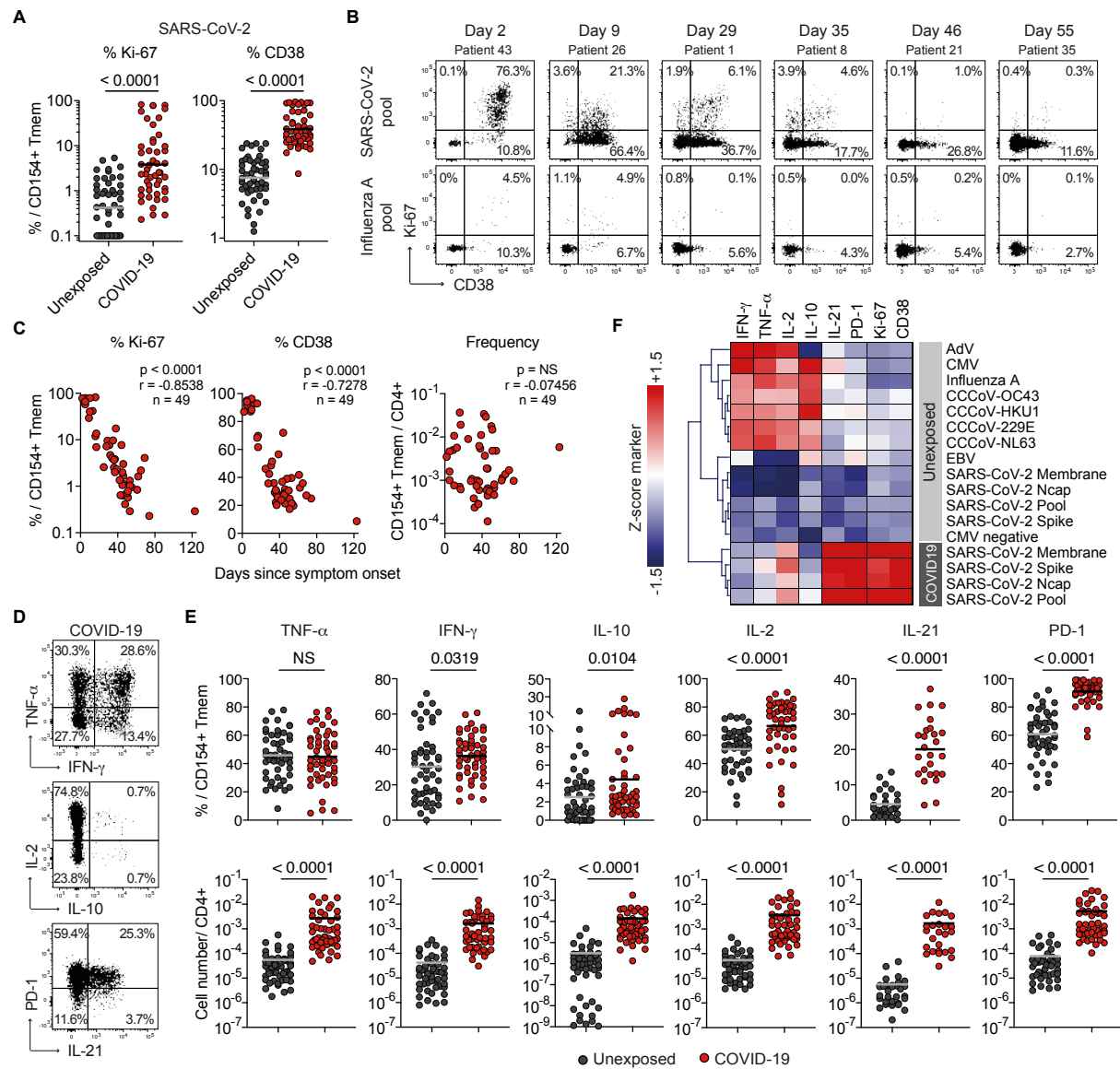


Figure 3

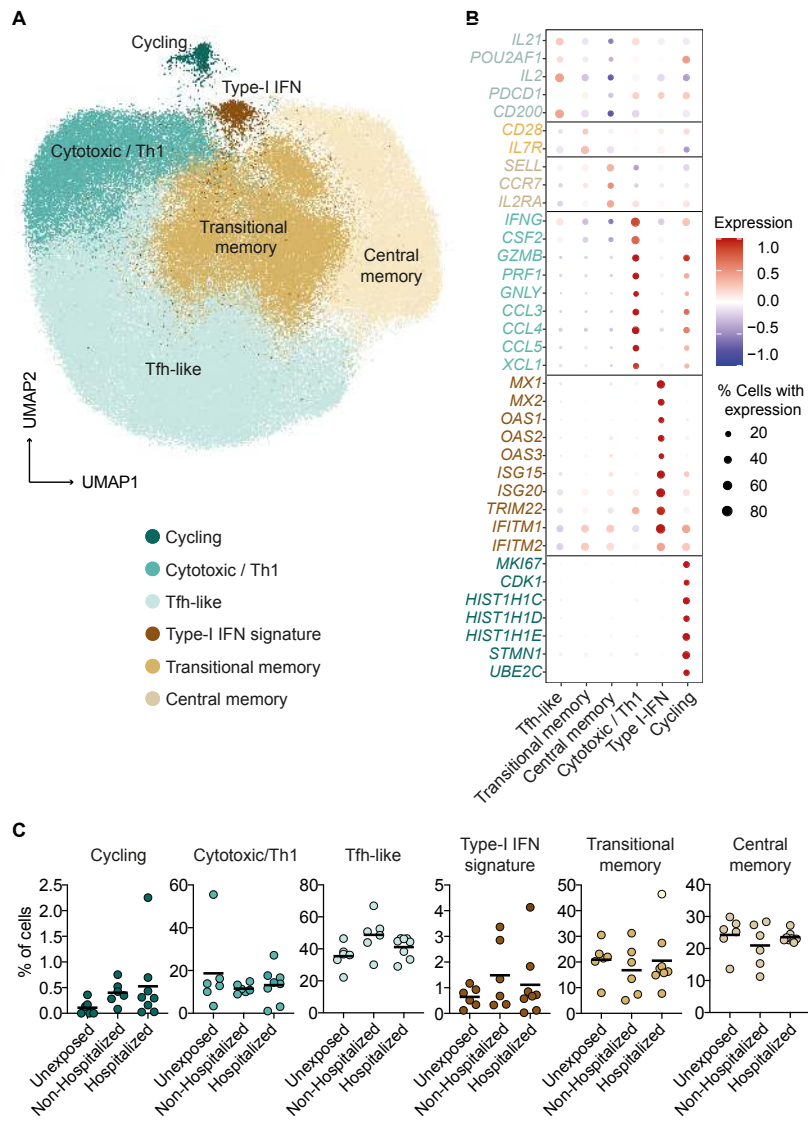


Figure 4

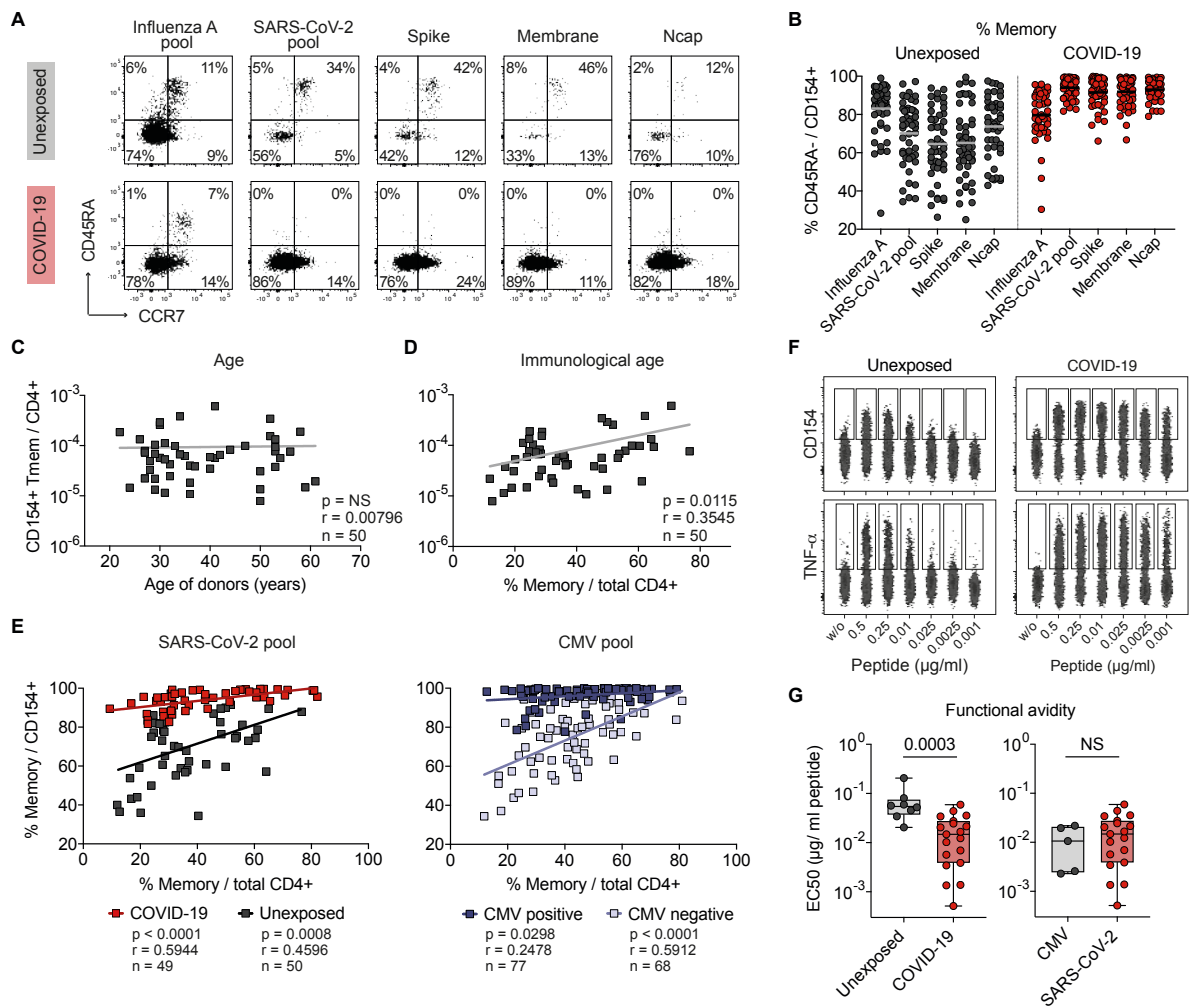


Figure 5

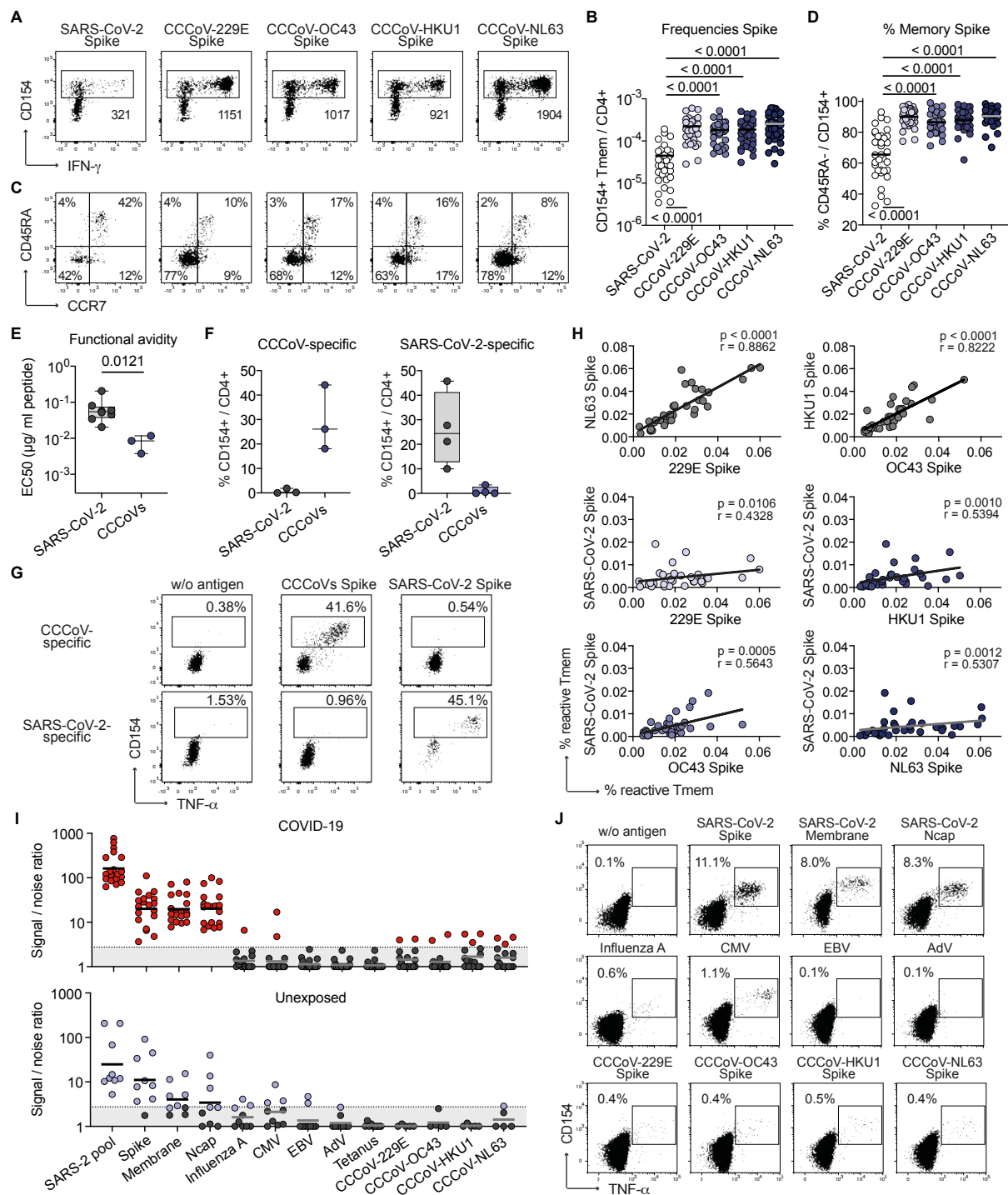


Figure 6

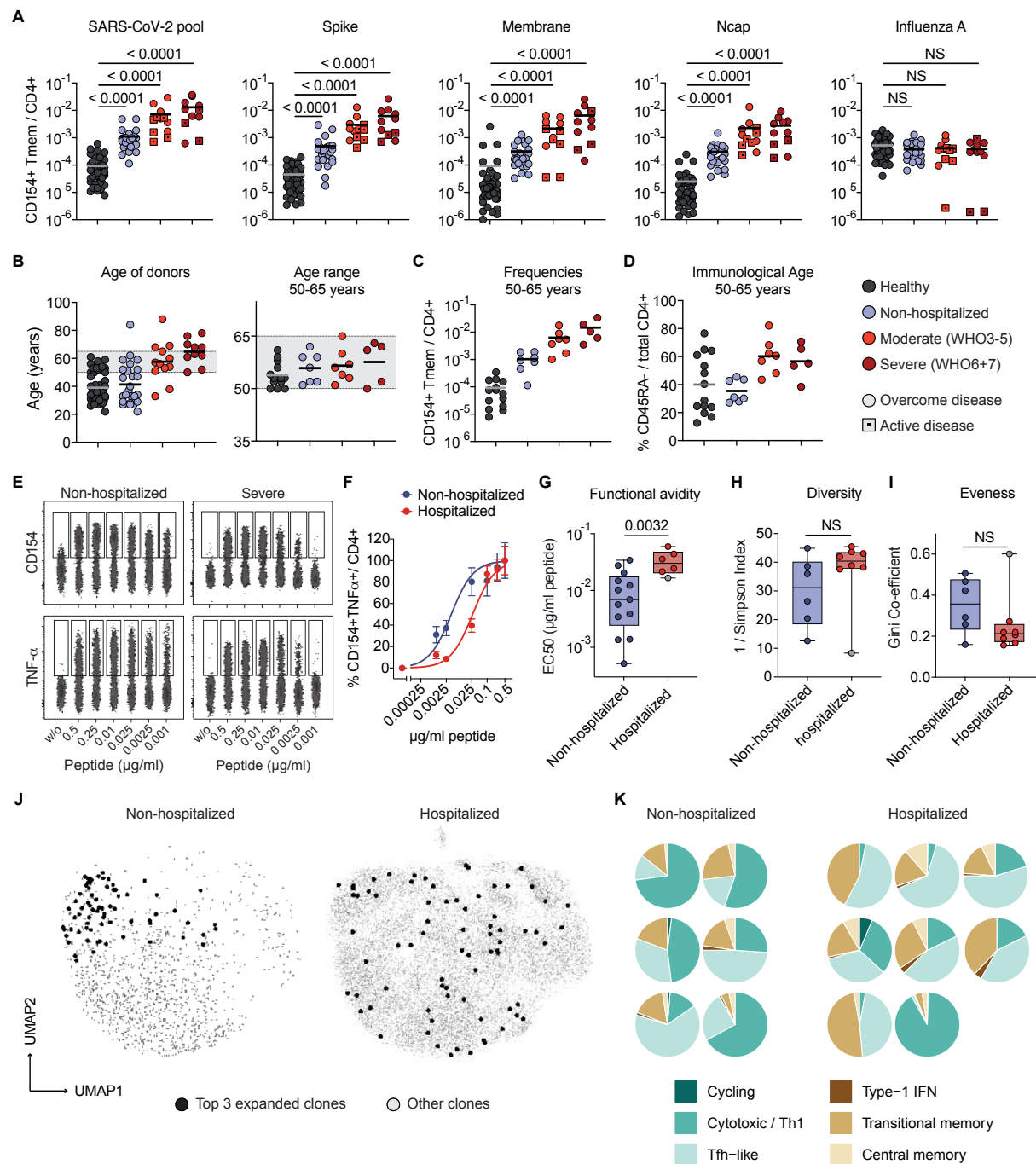


Figure S1

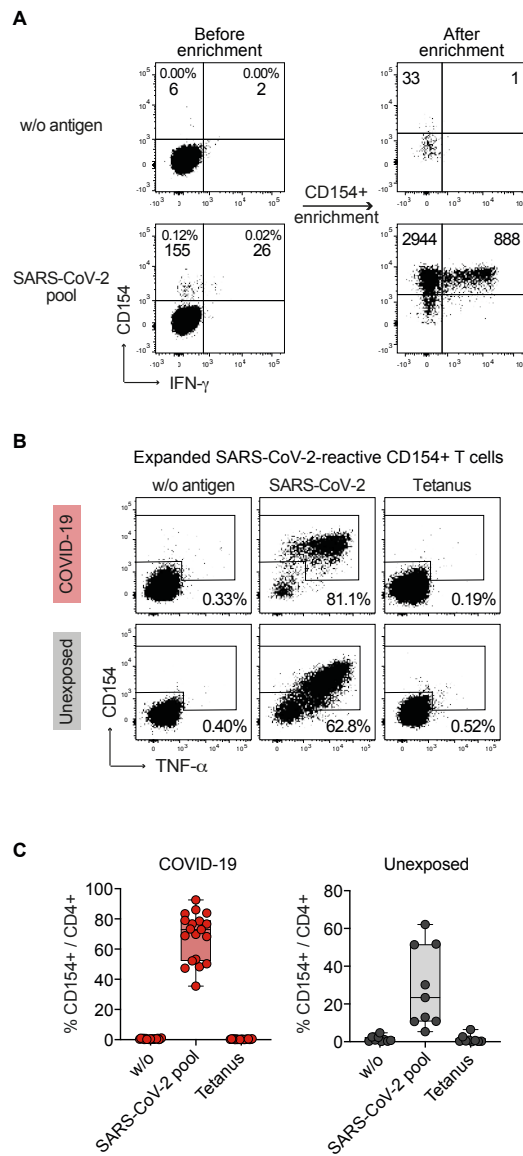


Figure S2

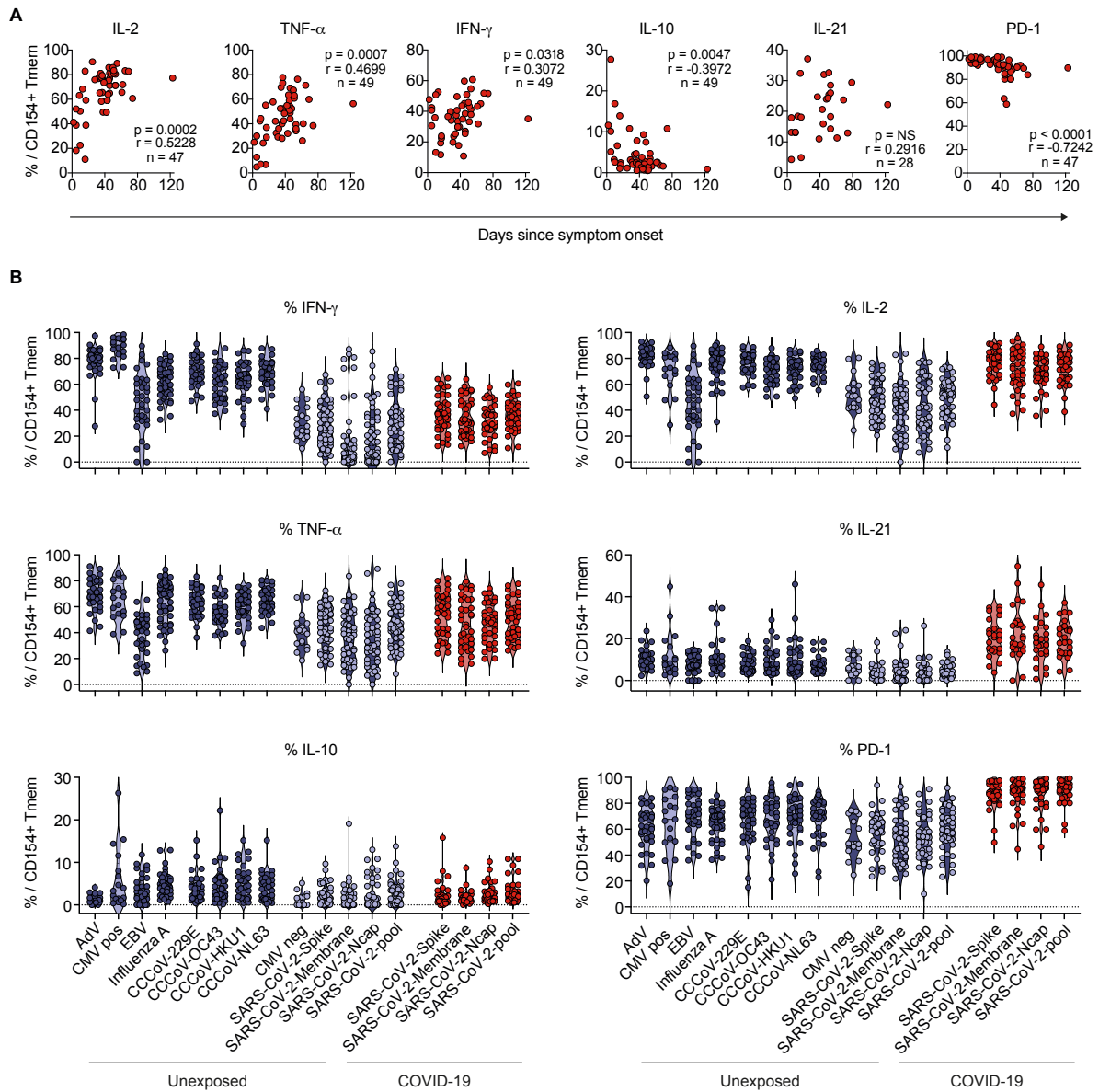


Figure S3

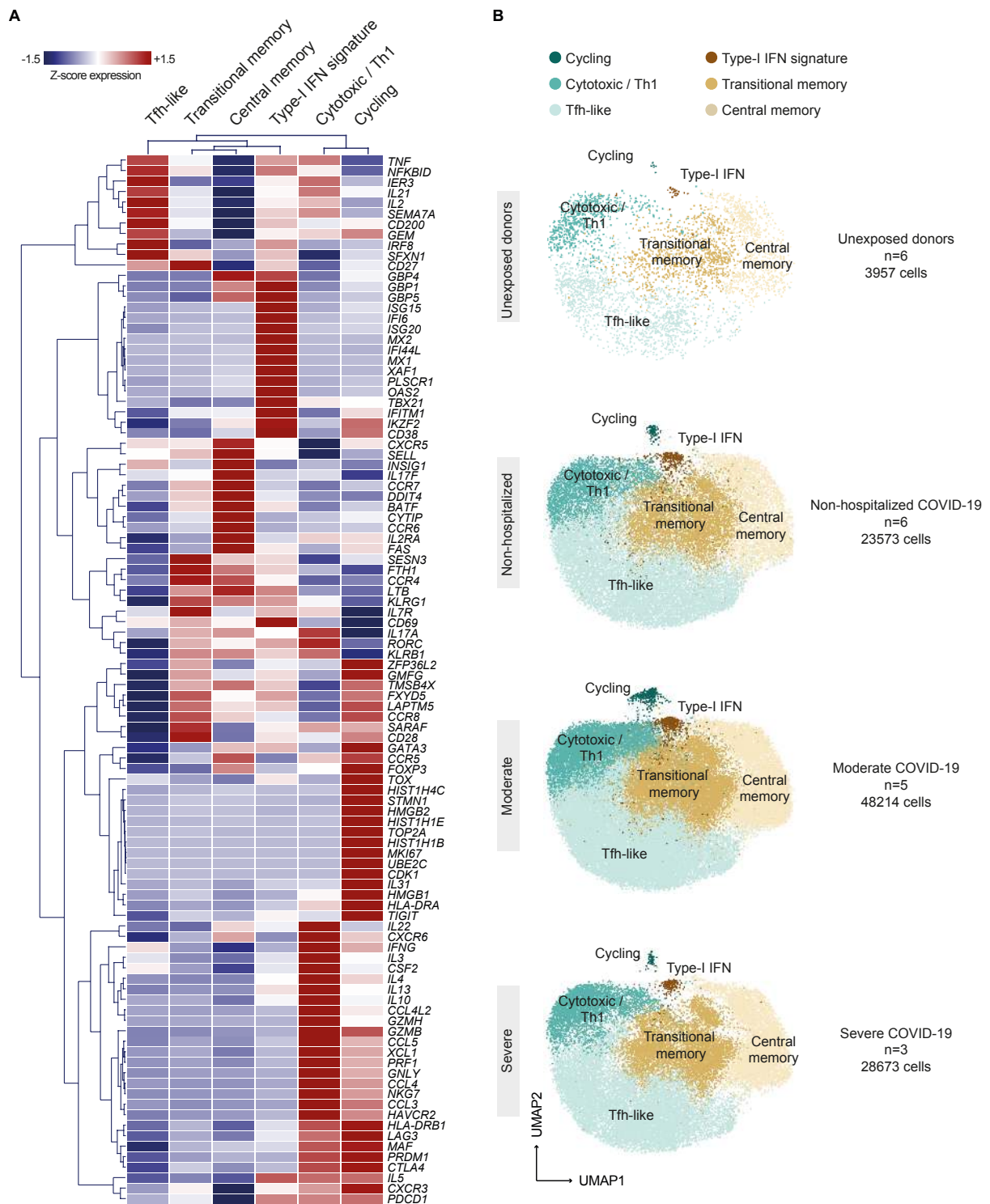


Figure S4

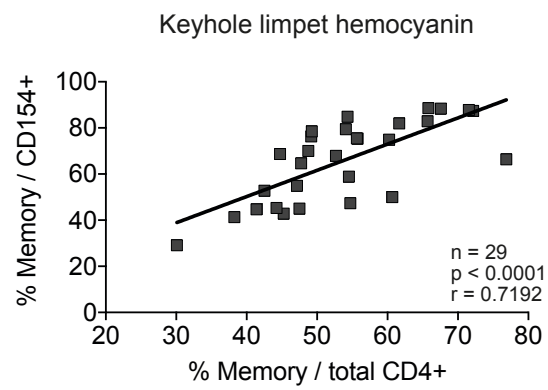


Figure S5

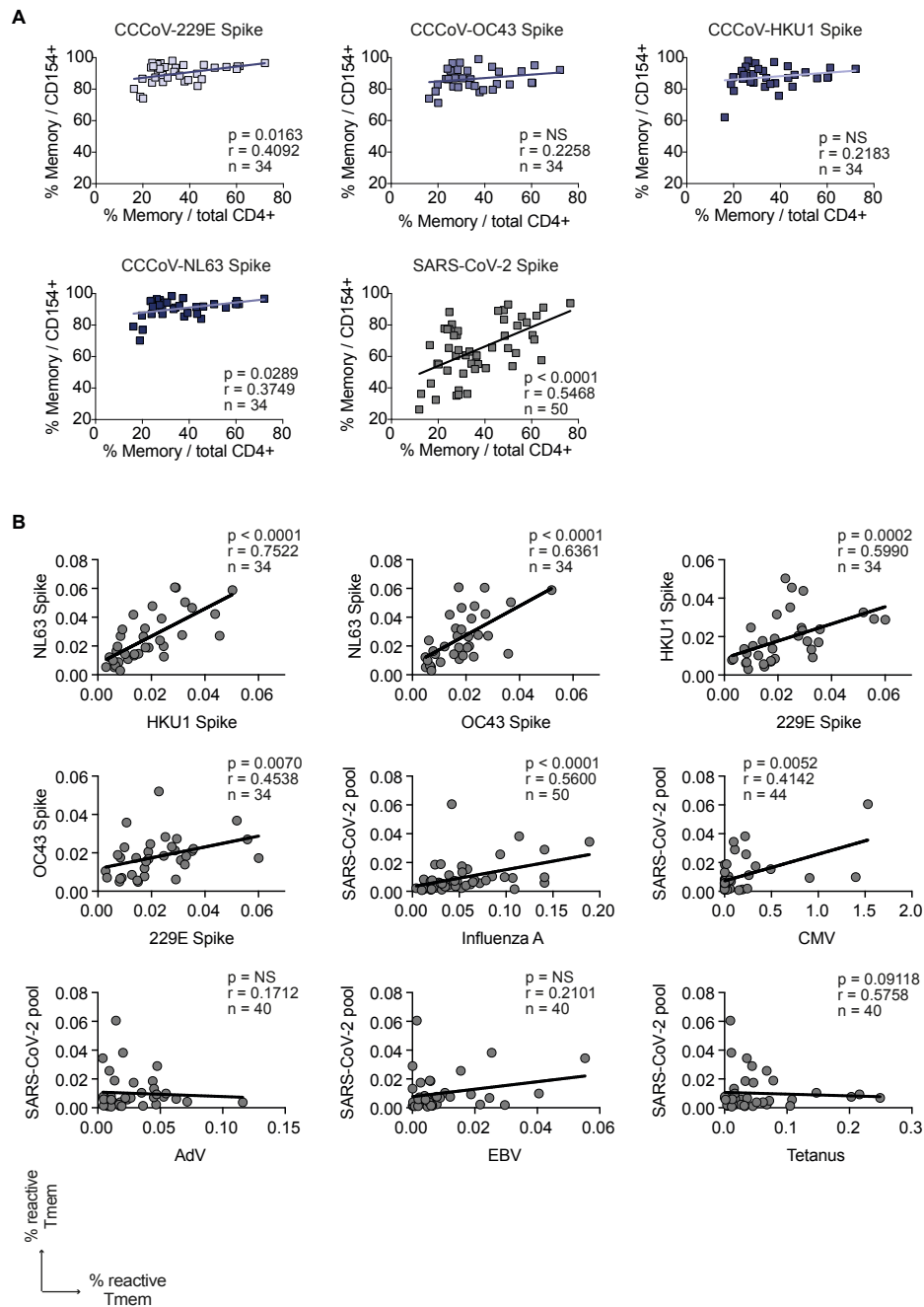


Figure S6

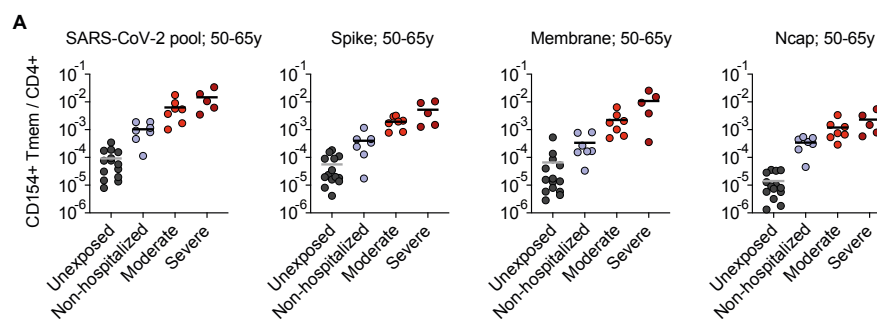


Table S1. Cohort characteristics

	COVID-19 (n=49)	Unexposed (n=50)
Age mean	51 years (range 22-88)	39 years (range 22-61)
Gender		
Male	53% (26/49)	32% (16/50)
Female	47% (23/49)	68% (34/50)
Disease Severity^a		
Non-hospitalized (WHO 1-2)	53% (26/49)	NA
Mild-moderate (WHO 3-5)	25% (12/49)	NA
Severe (WHO 6-7)	22% (11/49)	NA
SARS-CoV PCR positive		
Non-hospitalized (WHO 1-2)	81% (21/26)	NA
Mild-moderate (WHO 3-5)	100% (12/12)	NA
Severe (WHO 6-7)	100% (11/11)	NA
Total	90% (44/49)	NA
Antibody test positive^b		
Non-hospitalized (WHO 1-2)	100% (26/26)	NA
Mild-moderate (WHO 3-5) ^{b, c}	75% (9/12)	NA
Severe (WHO 6-7)	100% (11/11)	NA
Total	94% (46/49)	0% (0/50)

^a WHO criteria

^b Elecsys Anti-SARS-CoV-2, Roche Diagnostics GmbH

^c Anti-SARS-CoV-2 ELISA, Euroimmun

NA=not applicable